Stock assessment

2nd season 2017

Doryteuthis gahi

Andreas Winter

Natural Resources

Fisheries

November 2017

DESIRE THE RIGHT

Index

Summary

1) The 2017 second season *Doryteuthis gahi* fishery (X license) was open from July 29th, and closed by directed order on September 30th. Compensatory days for mechanical problems and bad weather resulted in 54 vessel-days taken after September 30th, with two vessels fishing as late as October 5th.

2) This season was characterized by an unusually abundant presence of pinnipeds *Arctocephalus australis* and *Otaria flavescens* in the fishing zone, and by the regulatory measures taken to mitigate mortality of these pinnipeds. *D. gahi* stock assessment was adjusted to the regulatory measures by shifting delineation between north and south assessment sub-areas from 52° S to 52.5° S latitude, and by applying depletion models with two independently optimized catchability coefficients for trawls taken with or without seal exclusion devices.

3) 24,101 tonnes of *D. gahi* catch were reported in the X-license fishery; the highest 2nd season catch since 2012 and giving an average CPUE of 24.05 t vessel-day^{-1}. During the season 29.8% of *D. gahi* catch and 48.2% of fishing effort were taken north of 52.5° S; 70.2% of *D. gahi* catch and 51.8% of fishing effort were taken south of 52.5° S.

4) Sub-areas north and south of 52°S were depletion-modelled separately. In the north sub-area, two depletion periods / immigrations were inferred to have started on August 5th and September 15th. In the south sub-area, two depletion periods / immigrations were inferred to have started on July 29th (start of the season) and September 15th.

5) Approximately 11,611 tonnes of *D. gahi* (95% confidence interval: [0 to 115,432] tonnes) were estimated to have immigrated into the Loligo Box during second season 2017, of which 4,908 t north of 52.5° S and 6,702 t south of 52.5° S.

6) The escapement biomass estimate for *D. gahi* remaining in the Loligo Box at the end of second season 2017 was:

   Maximum likelihood of 21,366 tonnes, with a 95% confidence interval of [9,984 to 114,362] tonnes.

   The risk of *D. gahi* escapement biomass at the end of the season being less than 10,000 tonnes was estimated at 2.5%.

Introduction

The second season of the 2017 *Doryteuthis gahi* fishery (Patagonian longfin squid – colloquially *Loligo*) opened on July 29th. Twelve X-licensed trawlers started the season on July 29th, while four trawlers delayed entry by 1 or 2 days for logistic requirements. During the season, 5 flex days were taken for mechanical repairs by various vessels. Every vessel took at least 1 bad-weather day for an unprecedented total of 47 bad-weather days (Figure 1). One vessel was assigned a day of experimental nearshore fishing for juvenile toothfish (*Dissostichus eleginoides*), and allocated a compensatory additional X-license day. The season ended by directed closure on September 30th. The various schedule adjustments amounted to 54 vessel-days being taken after September 30[th][a], with the last two vessels finishing on October 5th.

Total reported *D. gahi* catch under second season X license was 24,101 tonnes (Table 1), corresponding to an average CPUE of 24101 / 1002 = 24.05 tonnes vessel-day^{-1}. Catch and average CPUE was the highest in a second season since 2012.

---

[a] One vessel with a partial season allocation expended its flex days earlier than September 30th.
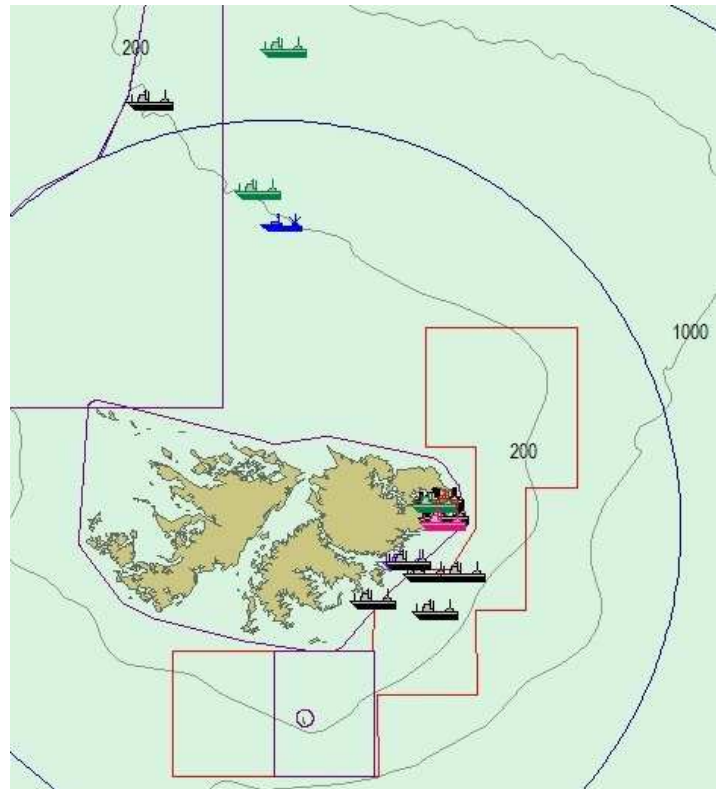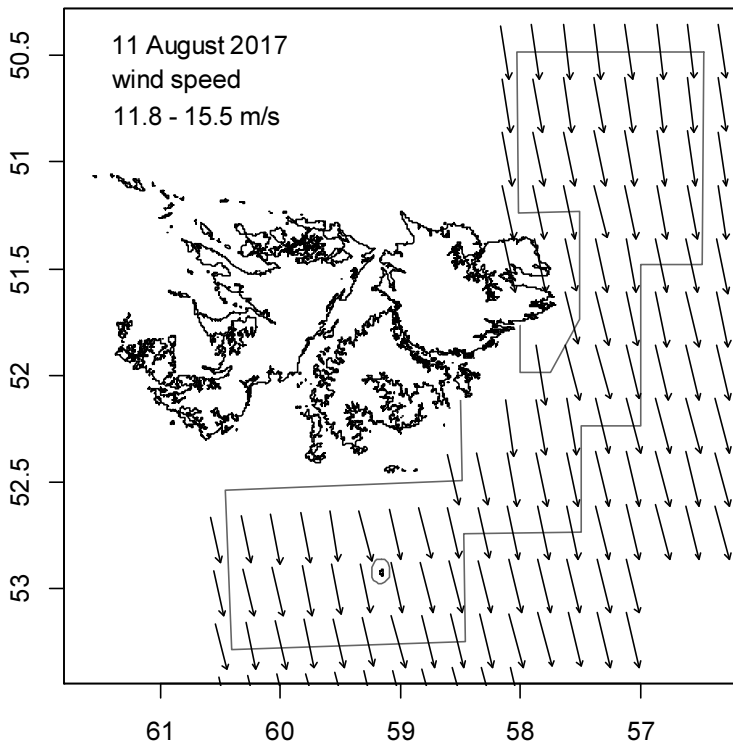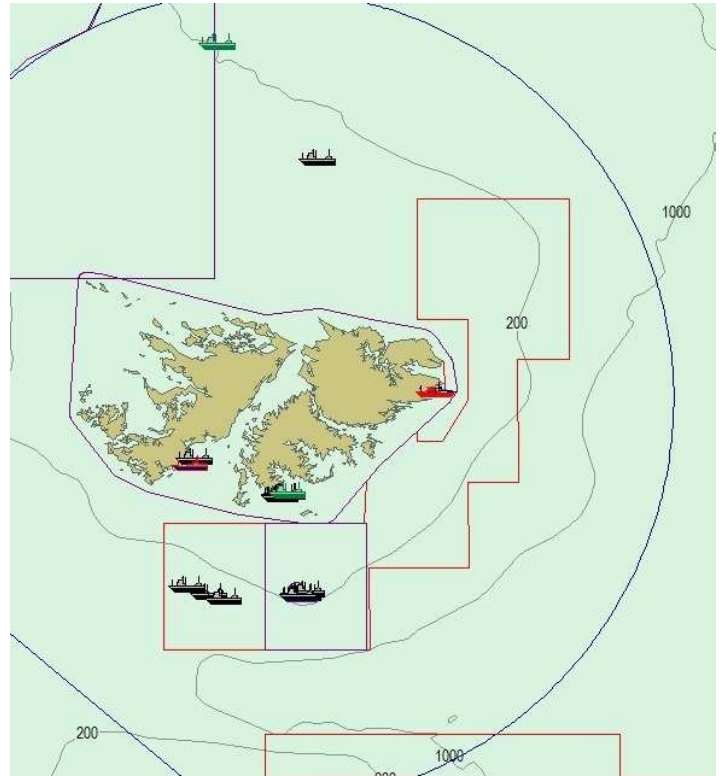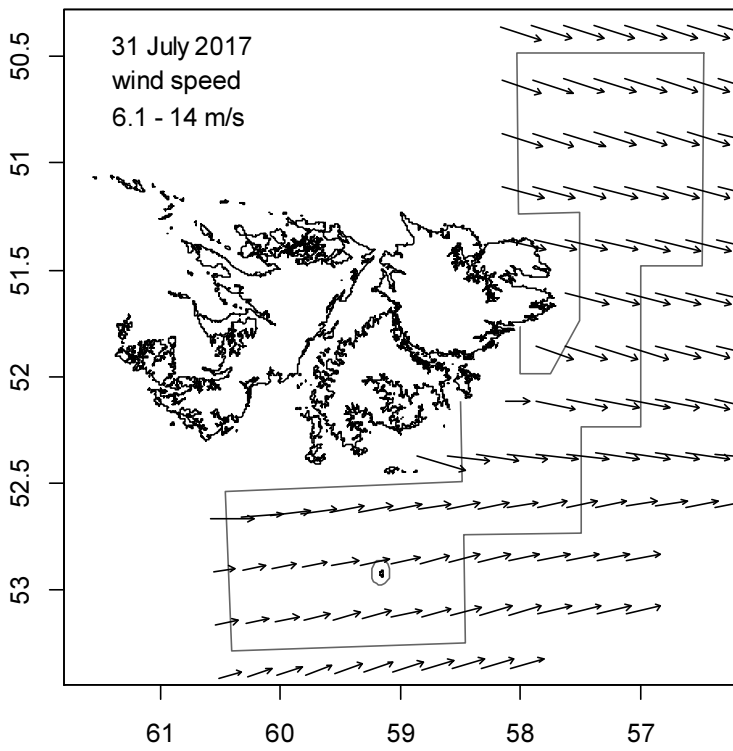
Figure 1. Left: wind speed vector plot at 0.25° resolution, from blended satellite observations (Zhang et al., 2006). Right: Fish Ops chart display. Top: July 31st, when 11 vessels declared bad-weather days, bottom: August 11th, when 14 vessels declared a bad-weather day.
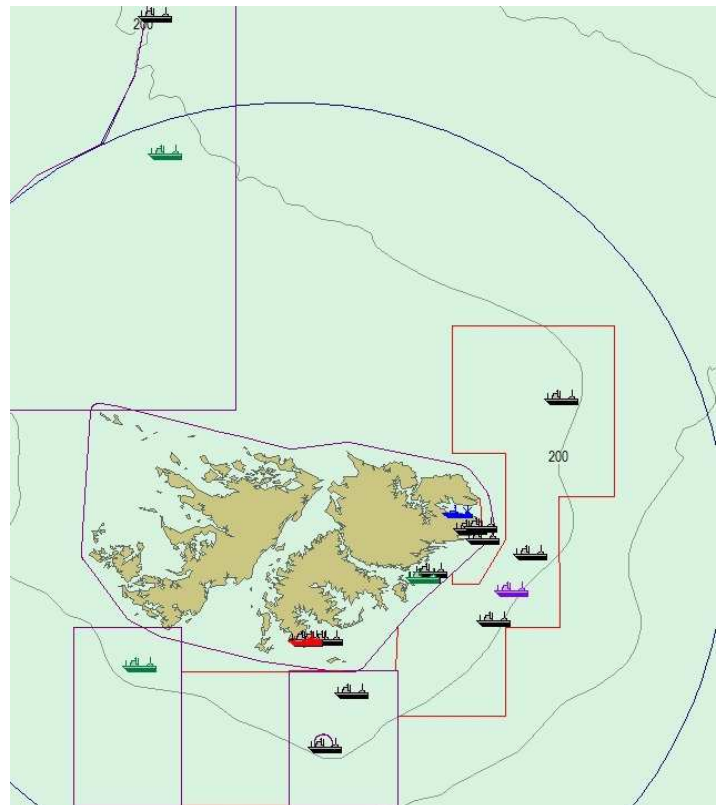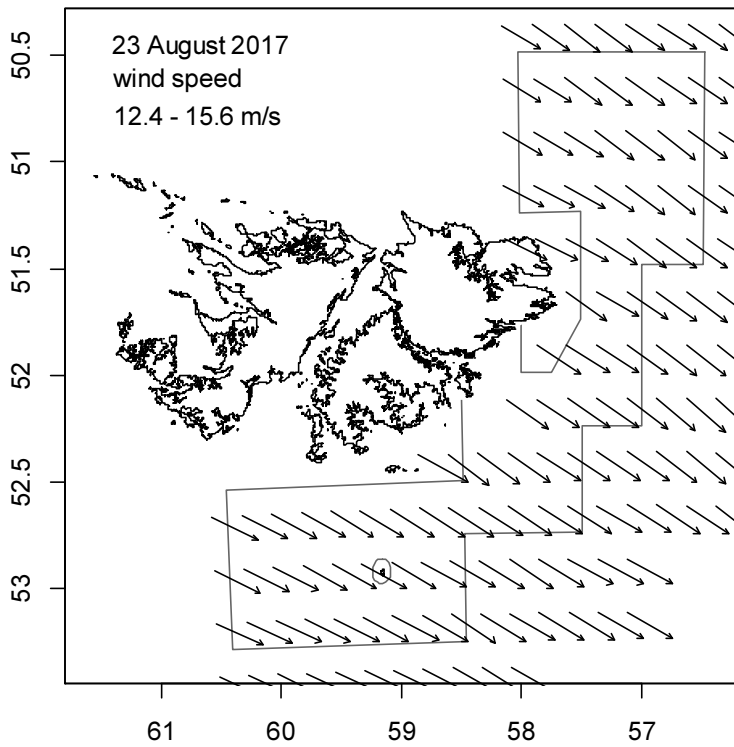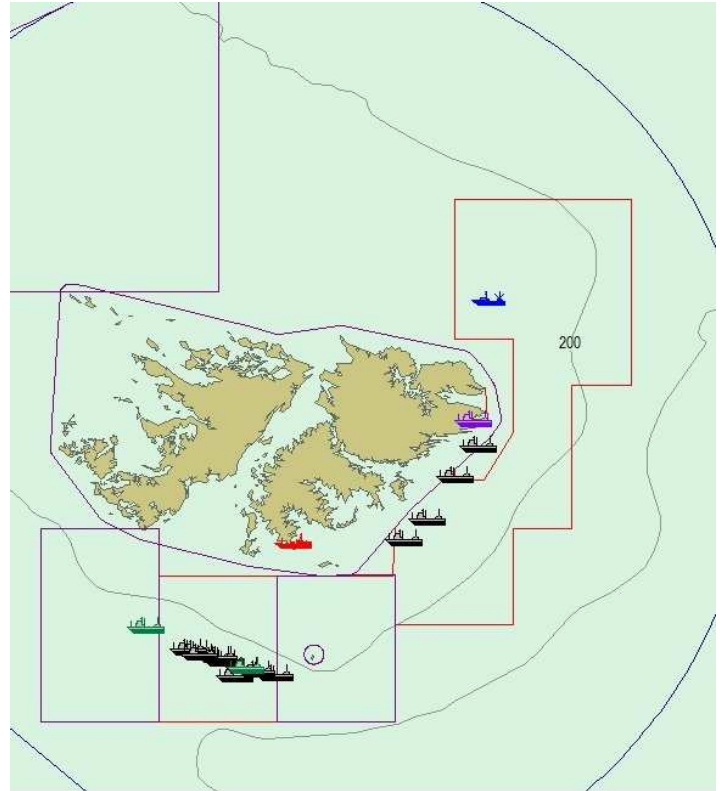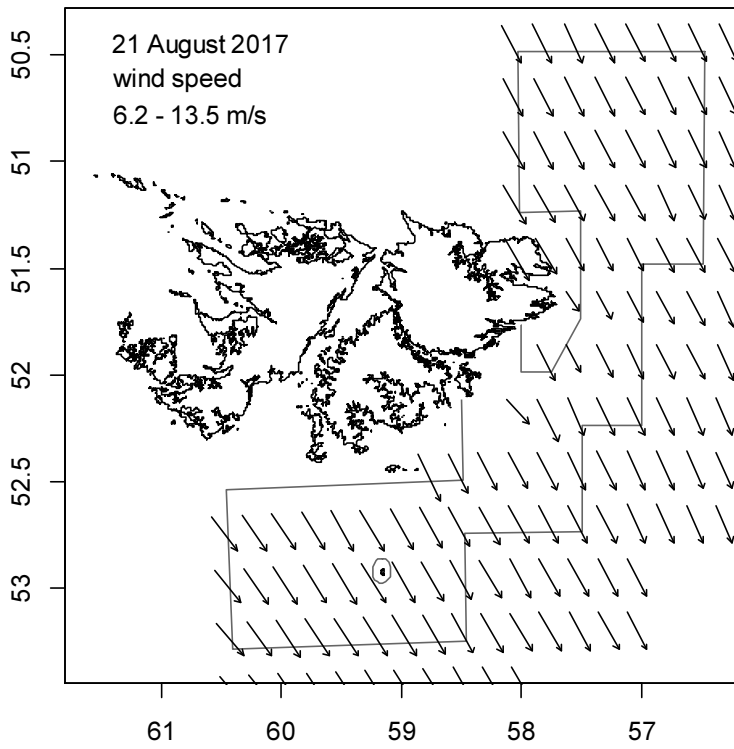
Figure 1 (continued). Top: August 21st, when 5 vessels declared bad-weather days, bottom: August 23rd, when 10 vessels declared a bad-weather day.

4
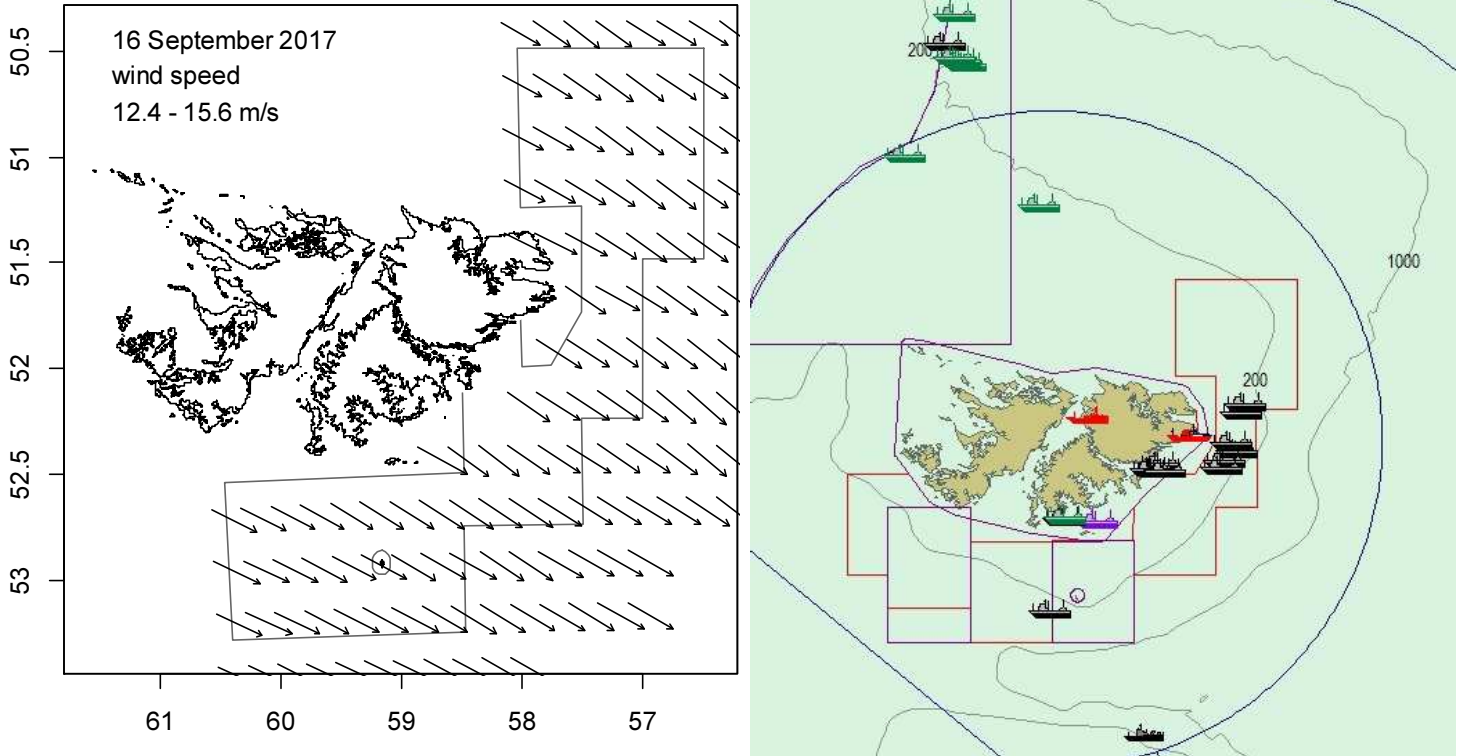
Figure 1 (concluded). September 16th, when 7 vessels declared a bad-weather day.

Assessment of the Falkland Islands *D. gahi* stock was conducted with depletion time-series models as in previous seasons (Agnew et al. 1998, Roa-Ureta and Arkhipkin 2007; Arkhipkin et al. 2008), and other squid fisheries (Royer et al. 2002, Young et al. 2004, Chen et al. 2008, Morales-Bojórquez et al. 2008, Keller et al. 2015, Medellín-Ortiz et al. 2016). Because *D. gahi* has an annual life cycle (Patterson 1988, Arkhipkin 1993), stock cannot be derived from a standing biomass carried over from prior years (Rosenberg et al. 1990, Pierce and Guerra 1994). The depletion model instead calculates an estimate of population abundance over time by evaluating what levels of abundance and catchability must be extant to sustain the observed rate of catch. Depletion modelling of the *D. gahi* target fishery is used both in-season and for the post-season summary, with the objective of maintaining an escapement biomass of 10,000 tonnes *D. gahi* at the end of each season as a conservation threshold (Agnew et al. 2002, Barton 2002).

Methods

The depletion model formulated for the Falklands *D. gahi* stock is based on the equivalence:

$$C_{day} = q \times E_{day} \times N_{day} \times e^{-M/2} \tag{1}$$

where q is the catchability coefficient, M is the natural mortality rate (considered constant at 0.0133 day^{-1}; Roa-Ureta and Arkhipkin 2007), and C_{day}, E_{day}, N_{day} are catch (numbers of squid), fishing effort (numbers of vessels), and abundance (numbers of squid) per day. In its

basic form (DeLury 1947) the depletion model assumes a closed population in a fixed area for the duration of the assessment. However, the assumption of a closed population is imperfectly met in the Falkland Islands fishery, where stock analyses have often shown that *D. gahi* groups arrive in successive waves after the start of the season (Roa-Ureta 2012; Winter and Arkhipkin 2015). Arrivals of successive groups are inferred from discontinuities in the catch data. Fishing on a single, closed cohort would be expected to yield gradually decreasing CPUE, but gradually increasing average individual sizes, as the squid grow. When instead these data change suddenly, or in contrast to expectation, the immigration of a new group to the population is indicated (Winter and Arkhipkin 2015).

Table 1. *D. gahi* season comparisons since 2004, when catch management was assumed by the FIFD. Days: total number of calendar days open to licensed *D. gahi* fishing including (since 1st season 2013) optional extension days; V-Days: aggregate number of licensed *D. gahi* fishing days reported by all vessels for the season. Entries in italics are seasons closed by emergency order.

	Season 1			Season 2		
	Catch (t)	Days	V-Days	Catch (t)	Days	V-Days
2004	7,152	46	625	17,559	78	1271
2005	24,605	45	576	29,659	78	1210
2006	19,056	50	704	*23,238*	*53*	*883*
2007	17,229	50	680	*24,171*	*63*	*1063*
2008	24,752	51	780	26,996	78	1189
2009	12,764	50	773	*17,836*	*59*	*923*
2010	28,754	50	765	36,993	78	1169
2011	15,271	50	771	*18,725*	*70*	*1099*
2012	34,767	51	770	35,026	78	1095
2013	19,908	53	782	19,614	78	1195
2014	28,119	59	872	19,630	71	1099
2015	*19,383**	*57**	*871**	*10,190*	*42*	*665*
2016	22,616	68	1020	23,089	68	1004
2017	39,433	68	999†	24,101	69	1002‡

* Does not include C-license catch or effort after the C-license target for that season was switched from *D. gahi* to *Illex*.
† Includes two vessel-days of experimental fishing for juvenile toothfish.
‡ Includes one vessel-day of experimental fishing for juvenile toothfish.

In the event of a new group arrival, the depletion calculation must be modified to account for this influx. This is done using a simultaneous algorithm that adds new arrivals on top of the stock previously present, and posits a common catchability coefficient for the entire depletion time-series. If two depletions are included in the same model (i.e., the stock present from the start plus a new group arrival), then:

$$C_{day} = q \times E_{day} \times (N1_{day} + (N2_{day} \times i2\big|_0^1)) \times e^{-M/2} \tag{2}$$

where i2 is a dummy variable taking the values 0 or 1 if 'day' is before or after the start day of the second depletion. For more than two depletions, $N3_{day}$, i3, $N4_{day}$, i4, etc., would be included following the same pattern.

A further modification to the depletion model was required in this season because of the abundant presence of pinnipeds (see Pinniped bycatch section). To mitigate the mortality

of pinniped interactions, fishing vessels were required to build seal exclusion devices (SEDs) into their trawl nets (Hamilton and Baker 2015), first for access to the southern sub-area and later throughout the entire fishing zone (Mercopress 2017a; 2017b). Because SEDs form a structural barrier within the net, trawls using SEDs present inherently different average catchability coefficients than trawls without SEDs. The depletion catch equation **2** was therefore formulated as the composite of fishing effort in parallel with and without SEDs (subscripts SED and NSED):

$$
\begin{aligned}
C_{day} \quad = \quad & q_{SED} \times E_{SED\text{-}day} \times (N1_{day} + (N2_{day} \times i2\vert_0^1)) \times e^{-M/2} \\
+ \quad & q_{NSED} \times E_{NSED\text{-}day} \times (N1_{day} + (N2_{day} \times i2\vert_0^1)) \times e^{-M/2}
\end{aligned}
\qquad \textbf{(3)}
$$

Either $E_{SED\text{-}day}$ or $E_{NSED\text{-}day}$ may $= 0$ on any day, in which case equation **3** defaults to equation **2**. Note however that equation **3** cannot be modelled as the simple addition of parallel SED and NSED catches ($C_{SED\text{-}day} + C_{NSED\text{-}day}$) because the squid abundance (N1 + N2 + …) is simultaneously targeted by both SED and NSED without distinction between SED and NSED. Two SED types were implemented during the season: a metal grill in front of the codend (termed "Lobitera"), and (briefly, by some vessels) a flexible mesh cover across the mouth of the trawl (termed "EuroRed" for its manufacturer). To keep the depletion model adequately simple, either was categorized as SED[b]; thus q_{SED} represents the average catchability of a pinniped-avoidance modified net[c]. Moreover, the computational difference between q_{SED} and q_{NSED} includes not only the technical efficacy of either gear but all fishing aspects that correlate with the gear; e.g., that vessels fishing under SED 'conditions' might also be taking shorter trawls than otherwise, or switching locations more frequently or distantly.

The season depletion likelihood function was calculated as the difference between actual catch numbers reported and catch numbers predicted from the model (Equation **3**), statistically corrected by a factor relating to the number of days of the depletion period (Roa-Ureta, 2012):

$$
((n\text{Days}\text{-}2)/2) \times \log\left(\sum_{days} (\log(\text{predicted}\,C_{day}) - \log(\text{actual}\,C_{day}))^2 \right)
\qquad \textbf{(4)}
$$

The stock assessment was set in a Bayesian framework (Punt and Hilborn 1997), whereby results of the season depletion model are conditioned by prior information on the stock; in this case the information from the pre-season survey.

The likelihood function of prior information was calculated as the normal distribution of the difference between catchability (q) derived from the survey abundance estimate, and catchability derived from the season depletion model. Catchability, rather than abundance N, is used for calculating prior likelihood because catchability informs the entire season time series; whereas N from the survey only informs the first in-season depletion period – subsequent immigrations and depletions are independent of the abundance that was present during the survey. In this season, only NSED fishing was conducted in the pre-season survey (Winter et al. 2017), and therefore only q_{NSED} could be linked to a prior. Thus, the prior likelihood function is:

---

[b] Also, a small number of trawls that tested both together.
[c] Which is not a conceptual departure for the model, as q always represents an average of catchabilities that actually vary among vessels and nets.

$$\frac{1}{\sqrt{2\pi \cdot SD_{q\ prior\ NSED}^2}} \times \exp\left(-\frac{\left(q_{model\ NSED} - q_{prior\ NSED}\right)^2}{2 \cdot SD_{q\ prior\ NSED}^2}\right) \tag{5}$$

where the standard deviation of catchability prior ($SD_{q\ prior\ NSED}$) is calculated from the Euclidean sum of the survey prior estimate uncertainty, the variability in catches on the season start date, and the uncertainty in the natural mortality M estimate over the number of days mortality discounting (Appendix: Equations **A5-N**, **A5-S**).

Bayesian optimization of the depletion was calculated by jointly minimizing Equations **4** and **5**, using the Nelder-Mead algorithm in R programming package 'optimx' (Nash and Varadhan 2011). Relative weights in the joint optimization were assigned to Equations **4** and **5** as the converse of their coefficients of variation (CV), i.e., the CV of the prior became the weight of the depletion model and the CV of the depletion model became the weight of the prior. Calculations of the CVs are described in Equations **A8-N** and **A8-S**. Because a complex model with multiple depletions may converge on a local minimum rather than global minimum, the optimization was stabilized by running a feed-back loop that set the q and N parameter outputs of the Bayesian joint optimization back into the in-season-only minimization (Equation **4**), re-calculated this minimization and the CV resulting from it, then re-calculated the Bayesian joint optimization, and continued this process until both the in-season minimization and the joint optimization remained unchanged.

With actual C_{day}, $E_{NSED - day}$, $E_{SED - day}$, and M being fixed parameters, the optimization of Equation **3** using Equations **4** and **5** produces estimates of q_{NSED}, q_{SED}, and N1, N2, …, etc. Numbers of squid on the final day (or any other day) of a time series are then calculated as the numbers N of the depletion start days discounted for natural mortality during the intervening period, and subtracting cumulative catch also discounted for natural mortality (CNMD). Taking for example a two-depletion period:

$$
\begin{aligned}
N_{final\ day} \quad = \quad & N1_{start\ day\ 1} \times e^{-M\ (final\ day - start\ day\ 1)} \\
& + N2_{start\ day\ 2} \times e^{-M\ (final\ day - start\ day\ 2)} \\
& - CNMD_{final\ day}
\end{aligned} \tag{6}
$$

where

$$CNMD_{day\ 1} \quad = \quad 0$$

$$CNMD_{day\ x} \quad = \quad CNMD_{day\ x-1} \times e^{-M} + C_{day\ x-1} \times e^{-M/2} \tag{7}$$

$N_{final\ day}$ is then multiplied by the average individual weight of squid on the final day to give biomass. Daily average individual weight is obtained from length / weight conversion of mantle lengths measured in-season by observers, and also derived from in-season commercial data as the proportion of product weight that vessels reported per market size category. Observer mantle lengths are scientifically accurate, but usually restricted to 1-2 vessels at any one time that may or may not be representative of the entire fleet, and not available every day. Commercially proportioned mantle lengths are relatively less accurate, but cover the entire fishing fleet every day. Therefore, both sources of data are used (see Appendix – *Doryteuthis gahi* individual weights).

Distributions of the likelihood estimates from joint optimization (i.e., measures of their statistical uncertainty) were computed using a Markov Chain Monte Carlo (MCMC) (Gamerman and Lopes 2006), a method that is commonly employed for fisheries assessments (Magnusson et al. 2013). MCMC is an iterative process which generates random stepwise changes to the proposed outcome of a model (in this case, the q and N of *D. gahi* squid) and

at each step, accepts or nullifies the change with a probability equivalent to how well the change fits the model parameters compared to the previous step. The resulting sequence of accepted or nullified changes (i.e., the 'chain') approximates the likelihood distribution of the model outcome. The MCMC of the depletion models were run for 200,000 iterations; the first 1000 iterations were discarded as burn-in sections (initial phases over which the algorithm stabilizes); and the chains were thinned by a factor equivalent to the maximum of either 5 or the inverse of the acceptance rate (e.g., if the acceptance rate was 12.5%, then every 8th (0.125^{-1}) iteration was retained) to reduce serial correlation. For each model three chains were run; one chain initiated with the parameter values obtained from the joint optimization of Equations **4** and **5**, one chain initiated with these parameters ×2, and one chain initiated with


Commercial catch, 29/07 - 05/10 2017
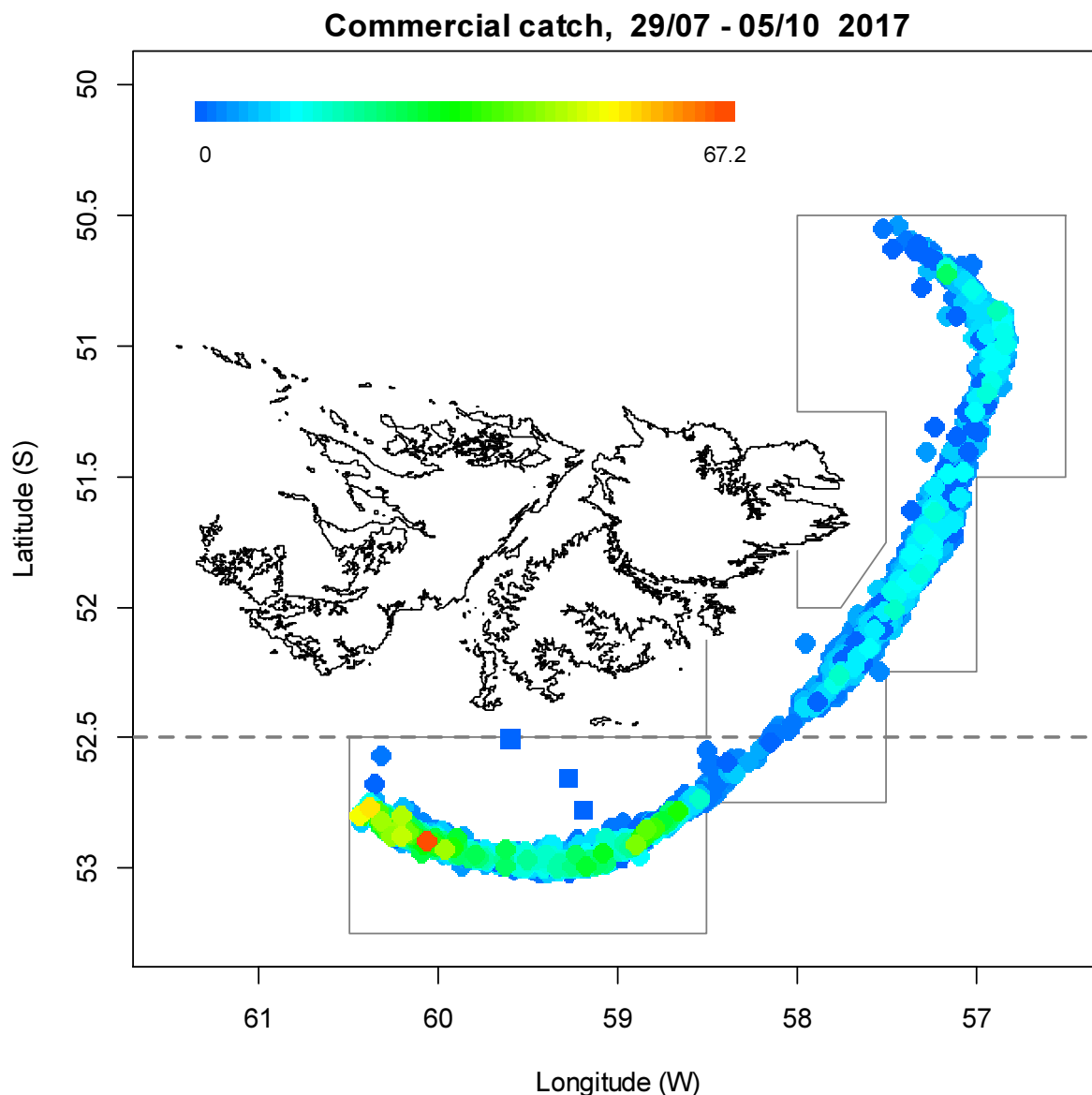
Figure 2. Spatial distribution of *D. gahi* 2nd-season trawls, colour-scaled to catch weight (max. = 67.2 tonnes). 3359 trawl catches were taken during the season. Trawls taken for juvenile toothfish experimental fishing are shown as squares. These toothfish trawls were under E licence, but are included as de facto in-season catches. The 'Loligo Box' fishing zone, as well as the 52.5 ºS parallel delineating the boundary between north and south assessment sub-areas, are shown in grey.

9

these parameters ×¼. Convergence of the three chains was accepted if the variance among chains was less than 10% higher than the variance within chains (Brooks and Gelman 1998). When convergence was satisfied the three chains were combined as one final set. Equations **6**, **7**, and the multiplication by average individual weight were applied to the CNMD and each iteration of N values in the final set, and the biomass outcomes from these calculations represent the distribution of the estimate. The peaks of the MCMC histograms were compared to the empirical optimizations of the N values.
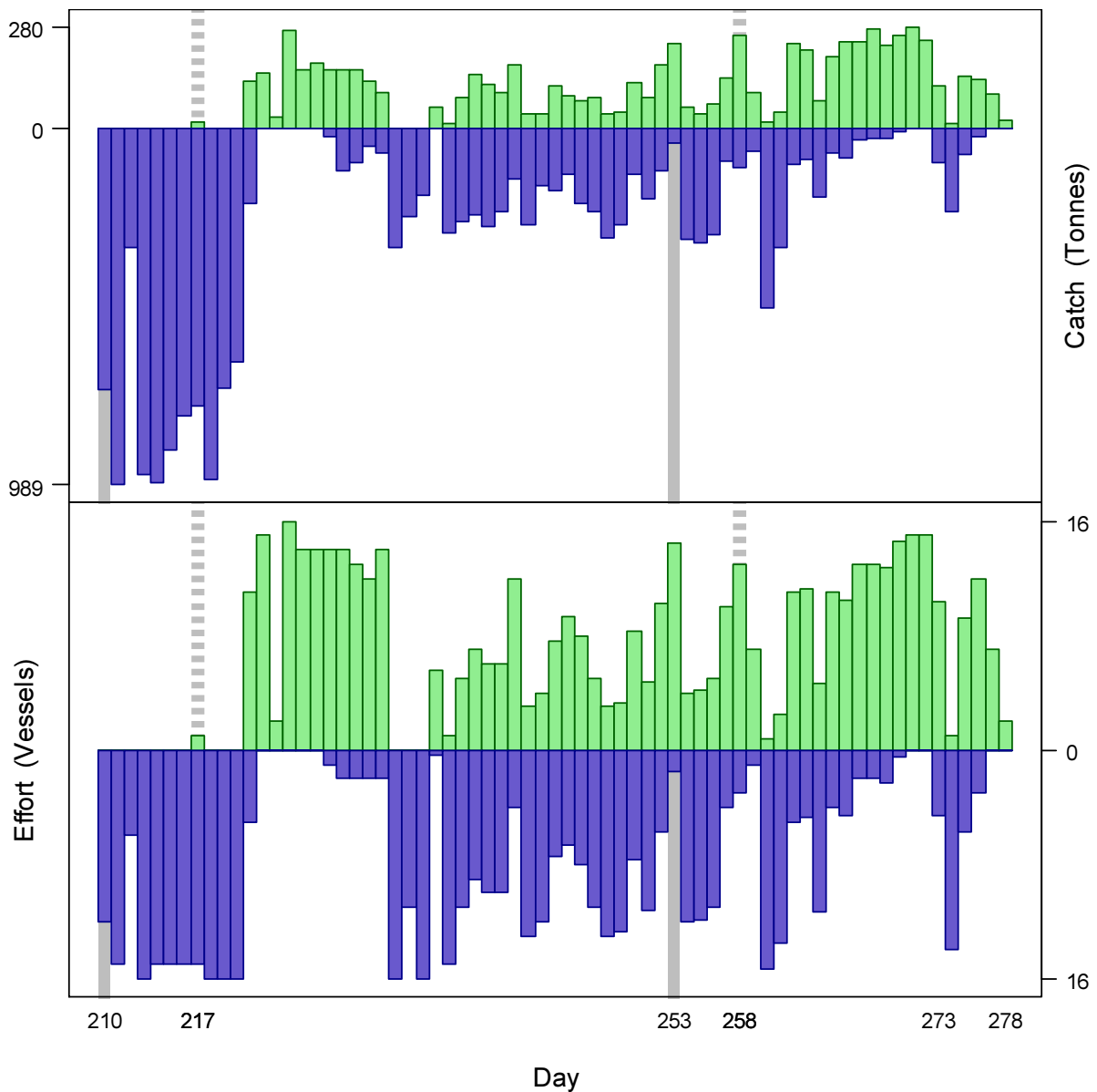

Figure 3. Daily total *D. gahi* catch and effort distribution by assessment sub-area north (green) and south (purple) of the 52.5° S parallel during 2nd season 2017. The season was open from July 29th (chronological day 210) to September 30th (chronological day 273), plus flex days until October 5th (day 278). As many as 16 vessels fished per day north of 52.5° S; as many as 16 vessels fished per day south of 52.5° S. As much as 280 tonnes *D. gahi* was caught per day north of 52.5° S; as much as 989 tonnes *D. gahi* was caught per day south of 52.5° S.

Depletion models and likelihood distributions were calculated separately for north and south sub-areas of the Loligo Box fishing zone, as *D. gahi* sub-stocks emigrate from different spawning grounds and remain to an extent segregated (Arkhipin and Middleton 2002). Total escapement biomass is then defined as the aggregate biomass of *D. gahi* on the last day of the season for north and south sub-areas combined. North and south biomasses are not assumed to be uncorrelated however (Shaw et al. 2004), and therefore north and south likelihood distributions were added semi-randomly in proportion to the strength of their day-to-day correlation (see Winter 2014, for the semi-randomization algorithm).

Stock assessment
Data

The conduct of the 2nd season was largely characterized by strategies to avoid pinniped bycatch, which had arisen in the pre-season survey as an exceptional issue (Winter et al. 2017). From the opening of the commercial season, an exclusion zone to the fishery was established from 52.5° S to 53.75° S latitude, and 59.5° W to 58.5° W longitude; an area surrounding Beauchêne Island where the highest numbers of pinniped mortalities had occurred in the pre-season survey (Winter et al. 2017). This exclusion was soon expanded to the entire Loligo Box south of 52.5° S latitude, with evidence that high pinniped mortalities were occurring throughout the south also further west. The south was subsequently re-opened to the fishery with the provision that vessels used nets fitted with SEDs and carried a FIG observer and / or contracted marine mammal monitor. To match data analyses with the fishing strategies of the season, the delineation between north and south assessment sub-areas was shifted from 52° S to 52.5° S latitude (Figure 2).

Fishing effort in the 2nd season 2017 started out concentrated in the south, where high catches were taken and higher abundances had been recorded in the pre-season survey (Winter et al. 2017). Following enactment of the expanded pinniped exclusion on August 10th vessels relocated north of 52.5° S, and were permitted to return south 10 days later once they met compliance with enhanced mitigation measures. Catches were variable from then on both north and south, but did not regain the same level as early in the season (Figure 3). Total fishing effort in the season was finally 48.2% in the north and 51.8% in the south, while total *D. gahi* catch was 29.8% in the north and 70.2% in the south.

1002 vessel-days were fished during the season (Table 1), with a median of 16 vessels per day (mean 14.52) except for flex and weather extensions. Vessels reported daily catch totals to the FIFD and electronic logbook data that included trawl times, positions, depths, and product weight by market size categories. Five FIG fishery observers were deployed on fifteen vessels in the fishing season for an exceptional total of 171 observer-days (Blake 2017, Boag 2017a; 2017b; 2017c, Derbyshire 2017a; 2017b; 2017c; 2017d, Huillier 2017a; 2017b; 2017c; 2017d; 2017e, Iriarte 2017a; 2017b; 2017c; 2017d). Throughout the 69 days of the season, 2 days had no observer covering (the bad weather day August 23rd (Figure 1), and the last extension day of the season when only two vessels still fished), 17 days had 1 observer covering, 17 days had two observers covering, 12 days had 3 observers covering, and 21 days had four observers covering. Throughout the season observers sampled an average of 325.5 *D. gahi* daily, and reported their maturity stages, sex, and lengths to 0.5 cm. The length-weight relationship for converting both observer and commercially proportioned length data was taken from the 2016 2nd pre-season survey (Winter et al. 2016), as the 2017 length-weight data were not available during the season:

weight (kg) $\quad = \quad 0.128 \times \text{length (cm)}^{2.322} / 1000$ **(8)**

In addition, the FIG seabird observer was deployed in the *D. gahi* fishery for 6 days on one vessel, and contractors were employed to monitor pinniped interactions for a total of 432 vessel-days: 11 days by two former FIG observers, 336 days by 12 MRAG contractors, 85 days by 4 CapFish contractors.

Group arrivals / depletion criteria

Start days of depletions - following arrivals of new *D. gahi* groups - were judged primarily by daily changes in CPUE, with additional information from sex proportions, maturity, and average individual squid sizes. CPUE was calculated as metric tonnes of *D. gahi* caught per vessel per day. Days were used rather than trawl hours as the basic unit of effort. Commercial vessels do not trawl standardized duration hours, but rather durations that best suit their daily processing requirements. An effort index of days is therefore more consistent.

Indicators of *D. gahi* immigration were relatively diffuse in this season because of the circumstance that vessels were required to fish *against* pinnipeds as much as fish *for* squid. Based on the available evidence, two days in the south and two days in the north were identified that represented the onset of separate *D. gahi* group arrivals / depletions.

- The first depletion south was identified on day 210 (July 29th – start of the commercial season) with 12 vessels entering the fishery in the south (Figure 3). CPUE was 60.3 t vessel[-1] day^{-1}, increasing to 65.9 t vessel[-1] day^{-1} the next day; highest CPUE of the season comprising more than a single vessel.
- The second depletion south was identified on day 253 (September 10th) after three consecutive days increasing CPUE (Figure 4), with a proportion of females that increased to its highest level in more than three weeks the day after (Figure 5C), and average maturities that suddenly decreased after an increasing trend since the beginning of the season (Figure 5D).
- The first depletion north was identified on day 217 (August 5th), the first day of any fishing in the north sub-area (by one vessel). Average commercial weights in the north were the lowest of the season on day 217 (Figure 5A).
- The second depletion north was identified on day 258 (September 15th) with an increase in CPUE to its highest level in 20 days (Figure 4).

13
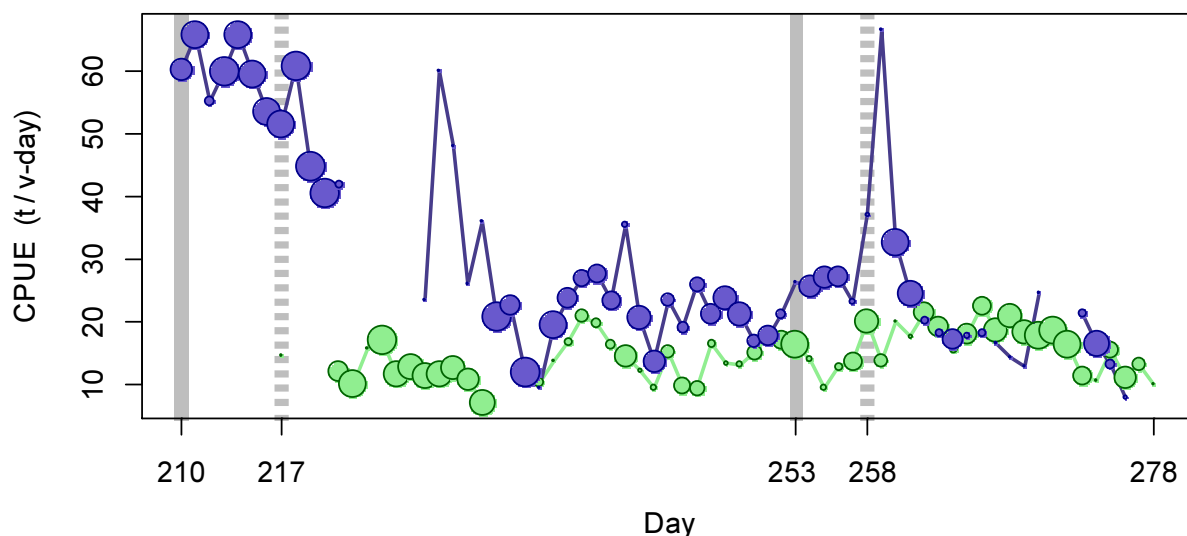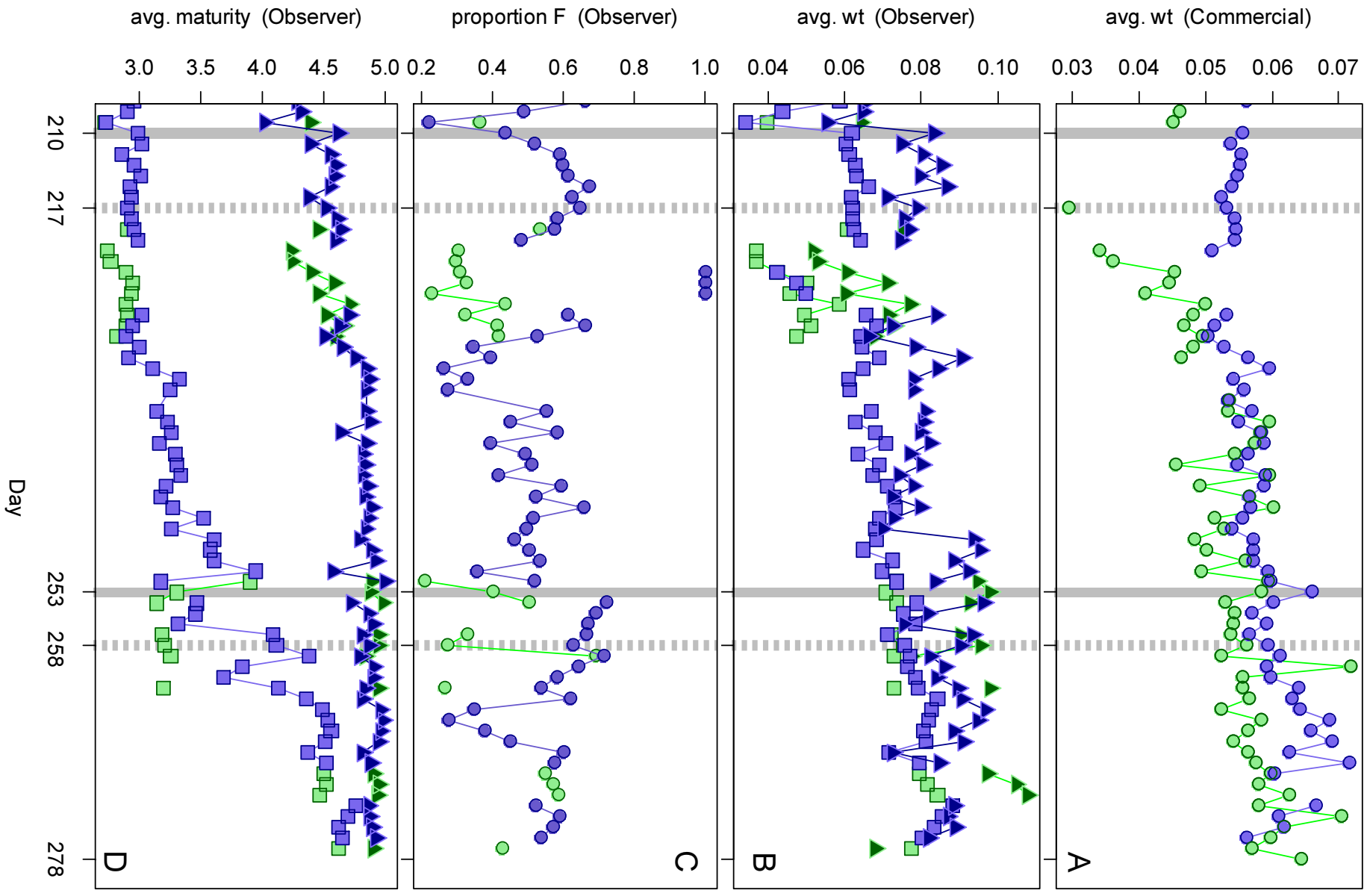
Figure 4 [preceding page]. CPUE in metric tonnes per vessel per day, by assessment sub-area north (green) and south (purple) of 52.5° S latitude. Circle sizes are proportioned to numbers of vessels fishing. Data from consecutive days are joined by line segments. Broken grey bars indicate the starts of in-season depletions north. Solid grey bars indicate the starts of in-season depletions south.

Figure 5 [previous page]. A: Average individual *D. gahi* weights (kg) per day from commercial size categories. B: Average individual *D. gahi* weights (kg) by sex per day from observer sampling. C: Proportions of female *D. gahi* per day from observer sampling. D: Average maturity value by sex per day from observer sampling. In all graphs – Males: triangles, females: squares, unsexed: circles. North sub-area: green, south sub-area: purple. Data from consecutive days are joined by line segments. Broken grey bars indicate the starts of in-season depletions north. Solid grey bars indicate the starts of in-season depletions south.

Depletion analyses
South

In the south sub-area, Bayesian optimization on catchability q without SEDs resulted in a maximum likelihood posterior ($_{\text{Bayesian}}$ q $_{\text{S NSED}}$ = 1.671 × 10^{-3}; Figure 6, left, and Equation **A9-S**) that was slightly higher than the pre-season prior ($_{\text{prior}}$ q $_{\text{S}}$ = 1.655 × 10^{-3}; Figure 6, left, and Equation **A4-S**) and lower than the in-season $_{\text{depletion}}$ q $_{\text{S NSED}}$ = 2.220 × 10^{-3} (Figure 6, left, and **A6-S**). Bayesian optimization was weighted as the converse of the CVs: 0.460 for in-season depletion (**A5-S**) vs. 0.491 for the prior (**A8-S**). With nearly even weights the posterior q distribution is expectedly closer to the prior than to the in-season depletion, as the prior is directly represented by the calculation of the q-values whereas in-season depletion is based on the catch / effort time series that simply uses q as a scaling value.


14
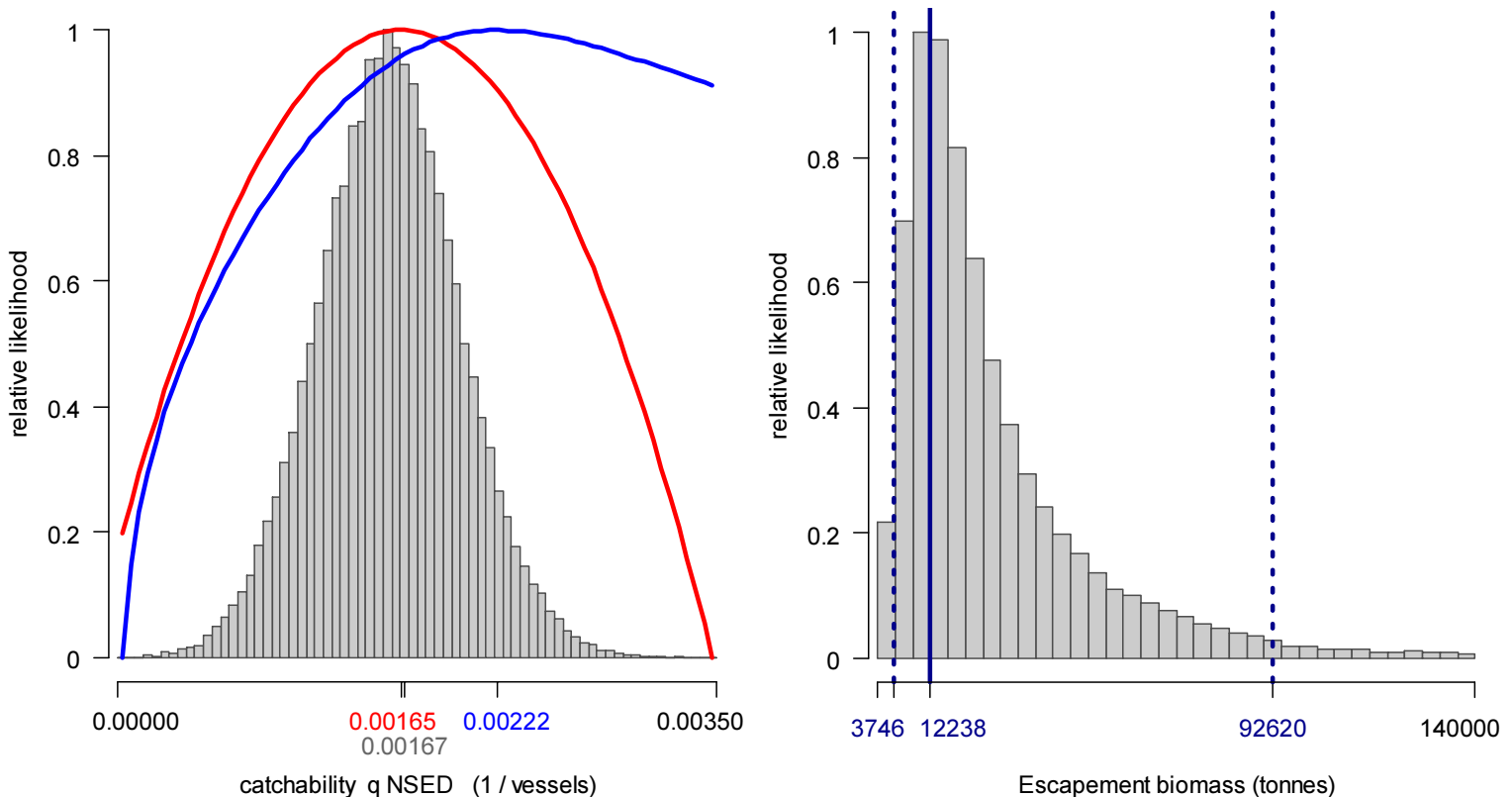
Figure 6 [previous page]. South sub-area. Left: Likelihood distributions for *D. gahi* NSED catchability. Red line: prior model (pre-season survey data), blue line: in-season depletion model, grey bars: combined Bayesian model posterior. Right: Likelihood distribution (grey bars) of escapement biomass, from the Bayesian posterior and average individual squid weight at the end of the season (day 278). Blue lines: maximum likelihood and 95% confidence interval. Note correspondence to Figure 7.
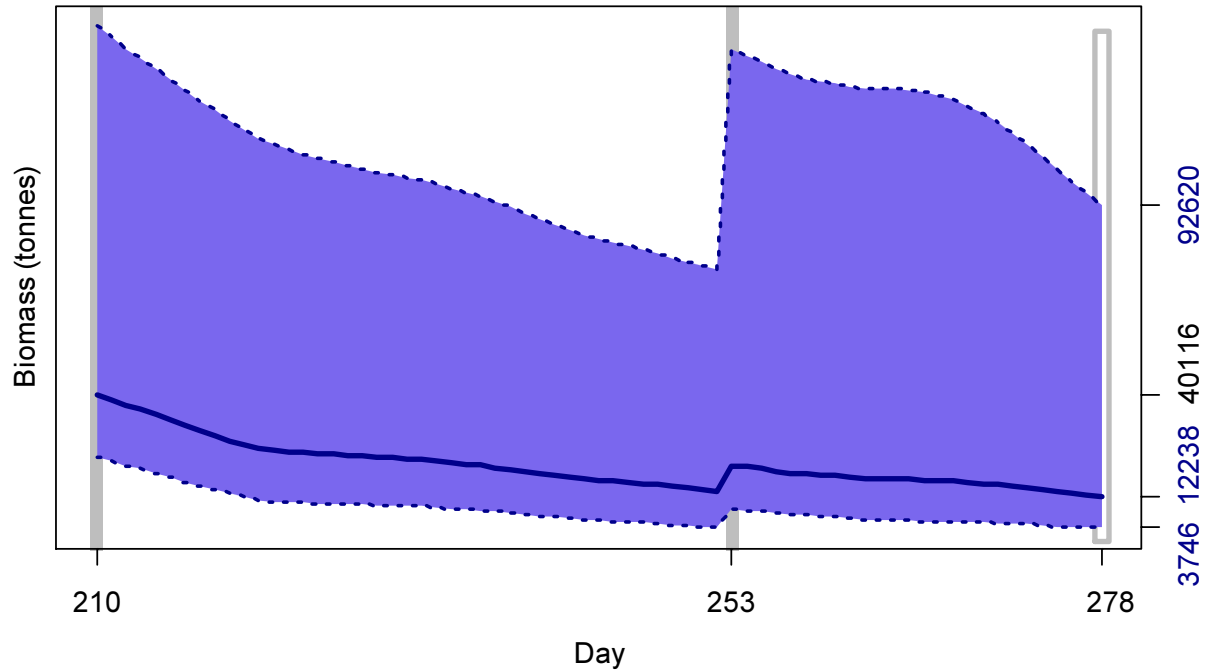

Figure 7. South sub-area. *D. gahi* biomass time series estimated from Bayesian posterior of the depletion model ± 95% confidence intervals. Gray bars indicate the start of in-season depletions south; days 210 and 253. Note that the biomass 'footprint' on day 278 (October 5th) corresponds to the right-side plot of Figure 6.

Posterior catchability with SEDs was $_{Bayesian}q_{S\,SED} = 1.217 \times 10^{-3}$ (Equation **A9-S**). The result implies that fishing with a SED in the net had $1.217 \times 10^{-3} / 1.671 \times 10^{-3} = 72.8\%$ of the squid catch efficacy of fishing without a SED.

The MCMC distribution of the Bayesian posterior multiplied by the GAM fit of average individual squid weight (Figure A1-south) gave the likelihood distribution of *D. gahi* biomass on day 278 (October 5th) shown in Figure 6-right, with maximum likelihood and 95% confidence interval of:

$$B_{S\,day\,278} \quad\quad = \quad 12{,}238\,t \sim 95\%\,CI\,[3{,}746 - 92{,}620]\,t \quad\quad\quad\quad (9)$$

At its highest point (on the first day of the season, day 210; July 29th), estimated *D. gahi* biomass south was 40,116 t ~ 95% CI [23,131 − 141,456] t (Figure 7). Variability remained high throughout the time period, and it is not statistically conclusive that any change in average biomass occurred during the season by the rule that a straight line could be drawn through the plot (Figure 7) without intersecting the 95% confidence intervals (Swartzman et al. 1992).

North

In the north sub-area, Bayesian optimization on catchability (q) without SEDs resulted in a maximum likelihood posterior of $_{\text{Bayesian}}q_{\text{N NSED}} = 0.881 \times 10^{-3}$ (Figure 8, left, and Equation **A9-N**). The pre-season prior was higher at $_{\text{prior}}q_N = 0.922 \times 10^{-3}$; Figure 8, left, and Equation **A4-N**) with a relatively broad distribution because of the high variability (Equation **A5-N**), while in-season depletion optimized lower at $_{\text{depletion}}q_{\text{N NSED}} = 0.780 \times 10^{-3}$ (Figure 8, left, and **A6-N**). Bayesian optimization was weighted as 0.827 for in-season depletion (**A5-N**) vs. 0.435 for the prior (**A8-N**).

Posterior catchability with SEDs was $_{\text{Bayesian}}q_{\text{N SED}} = 1.363 \times 10^{-3}$ (Equation **A9-S**). Counterintuitively, this implies that fishing with a SED in the net had higher squid catch efficacy than fishing without a SED: $1.363 \times 10^{-3} / 0.881 \times 10^{-3} = 154.7\%$. However, this is likely due to the constraints of the season. Vessels that fished north without an SED did so primarily because they were barred from the south, and fishing in the north only improved later in the season when all vessels had SEDs anyway. In effect, $q_{\text{N NSED}} = 0.881 \times 10^{-3}$ is the lowest since at least 2013, whereas $q_{\text{N SED}} = 1.363 \times 10^{-3}$ is not particularly high compared with other years.
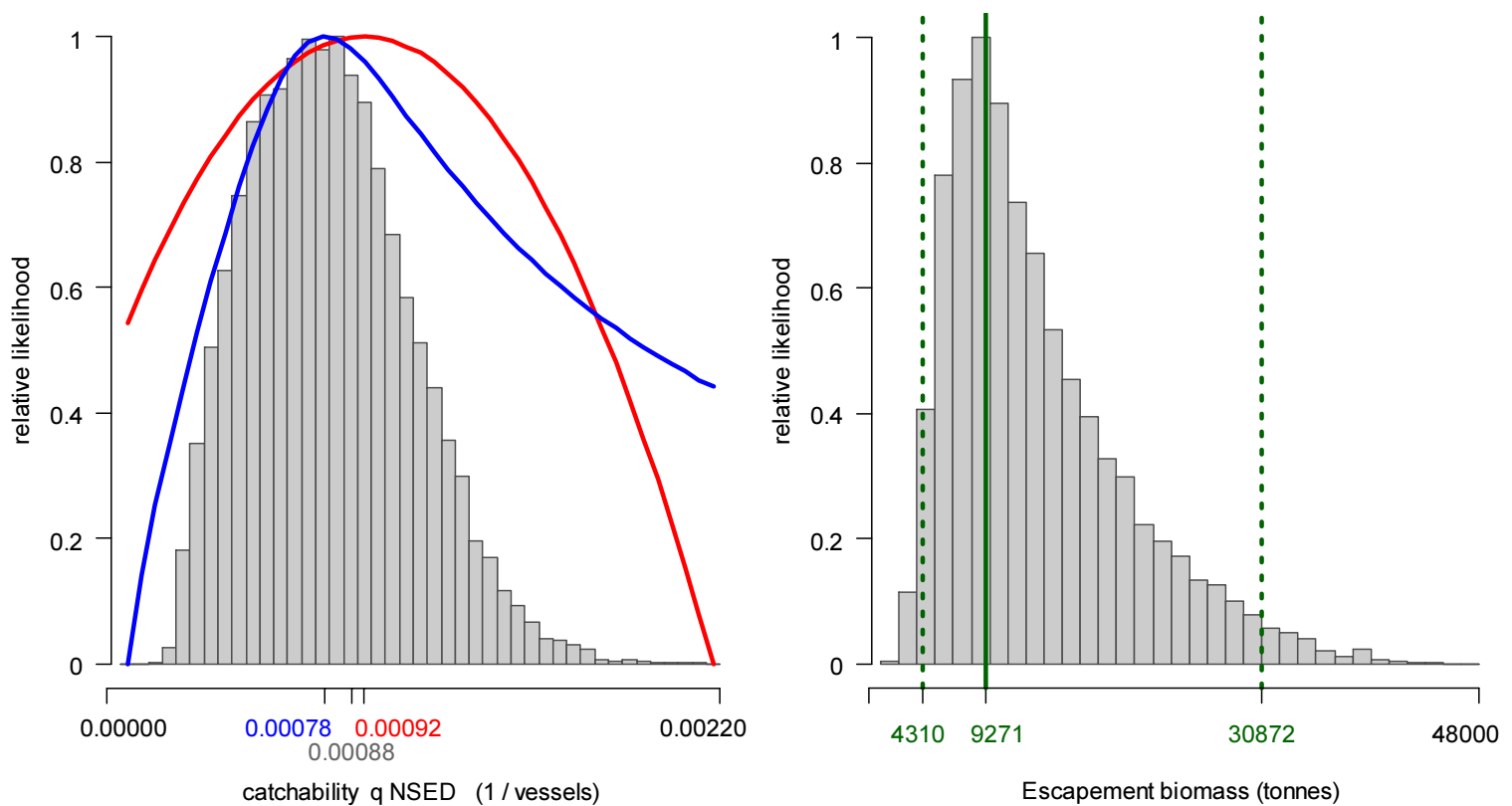
Figure 8. North sub-area. Left: Likelihood distributions for *D. gahi* NSED catchability. Red line: prior model (pre-season survey data), blue line: in-season depletion model, grey bars: combined Bayesian model posterior. Right: Likelihood distribution (grey bars) of escapement biomass, from Bayesian posterior and average individual squid weight at the end of the season. Green lines: maximum likelihood and 95% confidence interval. Note the correspondence to Figure 9.

The MCMC distribution of the Bayesian posterior multiplied by the GAM fit of average individual squid weight (Figure A1-north) gave the likelihood distribution of *D. gahi*

biomass on day 278 (October 5th) shown in Figure 8-right, with maximum likelihood and 95% confidence interval of:

$$B_{N \; day \; 278} \quad = \quad 9{,}271 \; t \; \sim \; 95\% \; CI \; [4{,}310 - 14{,}984] \; t \qquad \textbf{(10)}$$
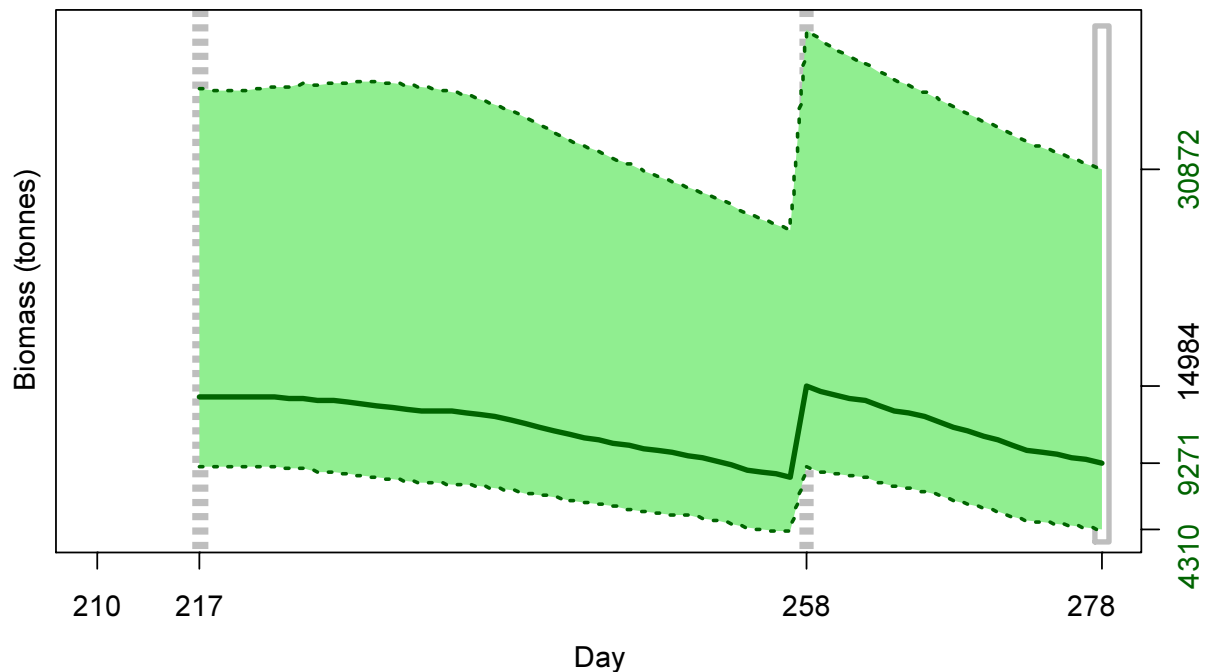
Figure 9. North sub-area. *D. gahi* biomass time series estimated from Bayesian posterior of the depletion model ± 95% confidence intervals. Broken grey bars indicate the start of in-season depletions north; days 217 and 258. Note that the biomass 'footprint' on day 278 (October 5th) corresponds to the right-side plot of Figure 8.

At its highest point (second depletion start: day 258 – September 15th), estimated *D. gahi* biomass north was 14,984 t ~ 95% CI [8,979 – 41,134] t (Figure 9). Like the south biomass time series (Figure 7), the north biomass time series (Figure 9) did not show statistically significant change over the duration of the season.

Escapement biomass

Total escapement biomass was defined as the aggregate biomass of *D. gahi* at the end of day 278 (October 5th) for north and south sub-areas combined (Equations **8** and **9**). Depletion models are calculated on the inference that all fishing and natural mortality are gathered at mid-day, thus a half day of mortality ($e^{-M/2}$) was added to correspond to the closure of the fishery at 23:59 (mid-night) on October 5th for the final two remaining vessels: Equation **10**. Semi-randomized addition of the north and south biomass estimates gave the aggregate likelihood distribution of total escapement biomass shown in Figure 10.

$$B_{Total \; day \; 278} \quad = \quad (B_{N \; day \; 278} \; + \; B_{S \; day \; 278}) \; \times \; e^{-M/2}$$

$$= \quad 21{,}509 \; t \; \times \; 0.9934$$

17

$$= \quad 21{,}366\,t \ \sim \ 95\% \ \text{CI} \ [9{,}984 - 114{,}362]\,t \qquad\qquad \textbf{(11)}$$

The risk of the fishery in the current season, defined as the proportion of the total escapement biomass distribution below the conservation limit of 10,000 tonnes (Agnew et al., 2002; Barton, 2002), was calculated as 2.51%.

The escapement biomass total of 21,366 tonnes was the median of the past five 2nd seasons, and above median of the past ten 2nd seasons. In contrast, season catch was highest of the past five 2nd seasons while slightly above median of the past ten 2nd seasons (Table 1), as catch and escapement tend not to show statistically significant correlations.
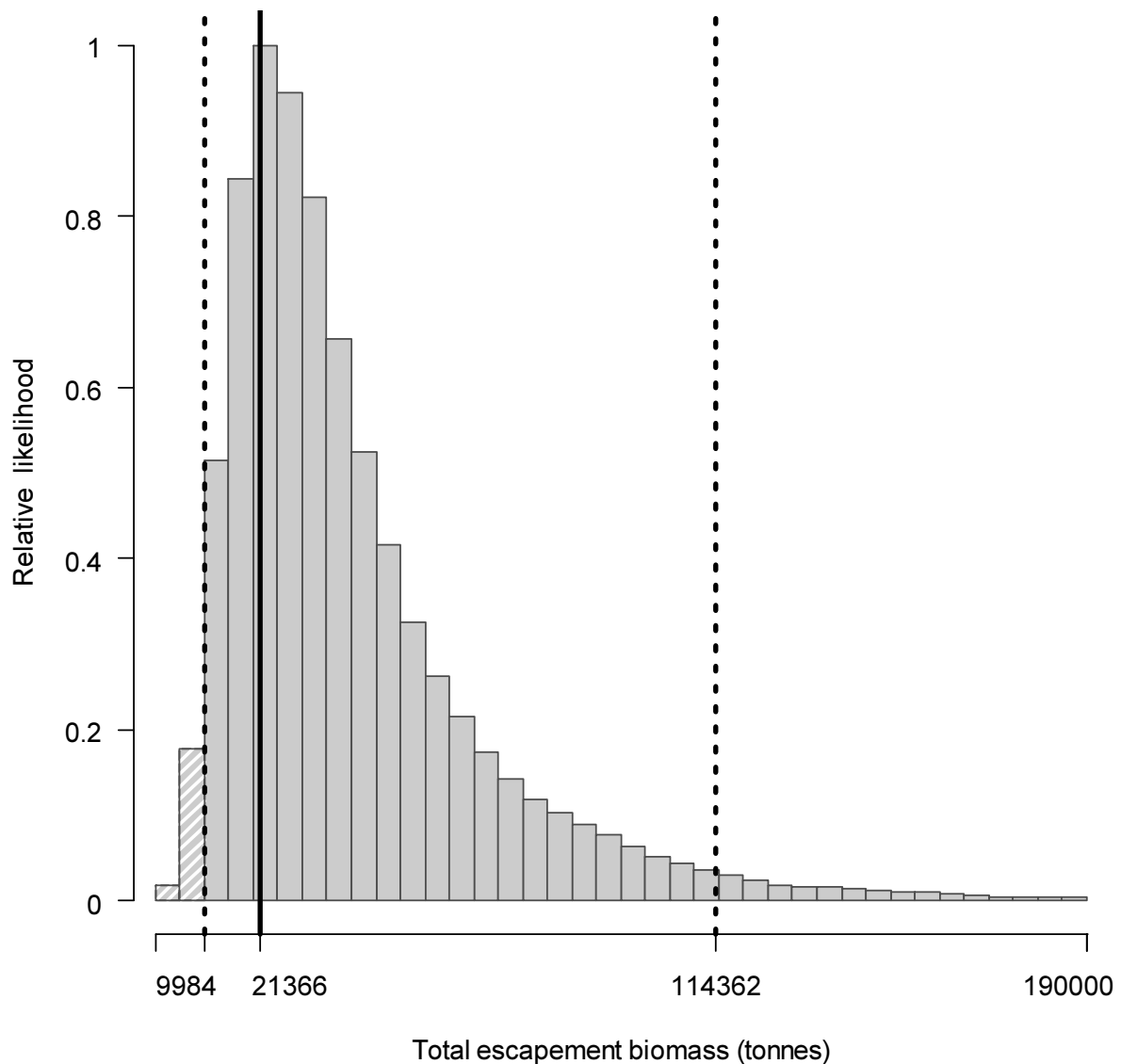
Figure 10. Likelihood distribution with 95% confidence intervals of total *D. gahi* escapement biomass at the season end (October 5th). White shading lines; portion of the distribution < 10,000 tonnes; equal to 2.51% of the whole distribution.

Immigration

Doryteuthis gahi immigration during the season was inferred on each day by how many more squid were estimated present than the day before, minus the number caught and the number expected to have died naturally; comparable to the equation for surplus production (Jacobson et al. 2002, Mueter and Megrey 2006):

$$\text{Immigration } N_{\text{day } i} = N_{\text{day } i} - (N_{\text{day } i-1} - C_{\text{day } i-1} - M_{\text{day } i-1})$$

where $N_{\text{day } i-1}$ are optimized in the depletion models, $C_{\text{day } i-1}$ calculated as in Equation **3**, and $M_{\text{day } i-1}$ is:

$$M_{\text{day } i-1} = (N_{\text{day } i-1} - C_{\text{day } i-1}) \times (1 - e^{-M})$$

Immigration biomass per day was then calculated as the immigration number per day multiplied by predicted average individual weight from the GAM:

$$\text{Immigration } B_{\text{day } i} = \text{Immigration } N_{\text{day } i} \times {}_{\text{GAM}} Wt_{\text{day } i}$$

All numbers N are themselves derived from the daily average individual weights, therefore the estimation automatically factors in that those squid immigrating on a given day would likely be smaller than average (because younger). Confidence intervals of the immigration estimates were calculated by applying the above algorithms to the MCMC iterations of the depletion models. Resulting total biomasses of *D. gahi* immigration north and south, up to season end (day 278), were:

$$\text{Immigration } B_{\text{N season}} = 4{,}908 \text{ t} \sim 95\% \text{ CI } [0 - 35{,}787] \text{ t} \qquad \textbf{(12-N)}$$

$$\text{Immigration } B_{\text{S season}} = 6{,}702 \text{ t} \sim 95\% \text{ CI } [0 - 91{,}535] \text{ t} \qquad \textbf{(12-S)}$$

Total immigration with semi-randomized addition of the confidence intervals was:

$$\text{Immigration } B_{\text{Total season}} = 11{,}611 \text{ t} \sim 95\% \text{ CI } [0 - 115{,}432] \text{ t} \qquad \textbf{(12-T)}$$

In the north sub-area, the in-season peak on day 258 accounted for approximately 94.6% of in-season immigration (start day 217 was de facto not an in-season immigration), consistent with the variation in time series biomass on Figure 9. In the south sub-area, the in-season peak on day 253 accounted for approximately 88.5% of in-season immigration (Figure 7).

Pinniped bycatch

Pinniped bycatch during 2nd season 2017 ultimately totalled 142 animals reported killed; 132 South American fur seals *Arctocephalus australis*, 9 Southern sea lions *Otaria flavescens*, and 1 species unidentified. Additionally, 286 South American fur seals, 7 Southern sea lions, and 1 unidentified pinniped were reported caught alive and released.

Several analyses were undertaken to examine distributions of pinniped bycatch relative to the fishery (Figure 11). The 418 (dead or alive) South American fur seals were taken within 182 of the 1002 vessel-days (Table 1), a highly significant aggregation (p < 0.0001 by randomization test). The 16 Southern sea lions were taken within 14 of the 1002

vessel-days, statistically neither aggregated nor dispersed (0.10 < p < 0.90). Fur seals and sea lions were never taken in the same trawl; dead or alive. Whether the two species were statistically avoidant of each other was marginally significant (p = 0.075 by permutation test).
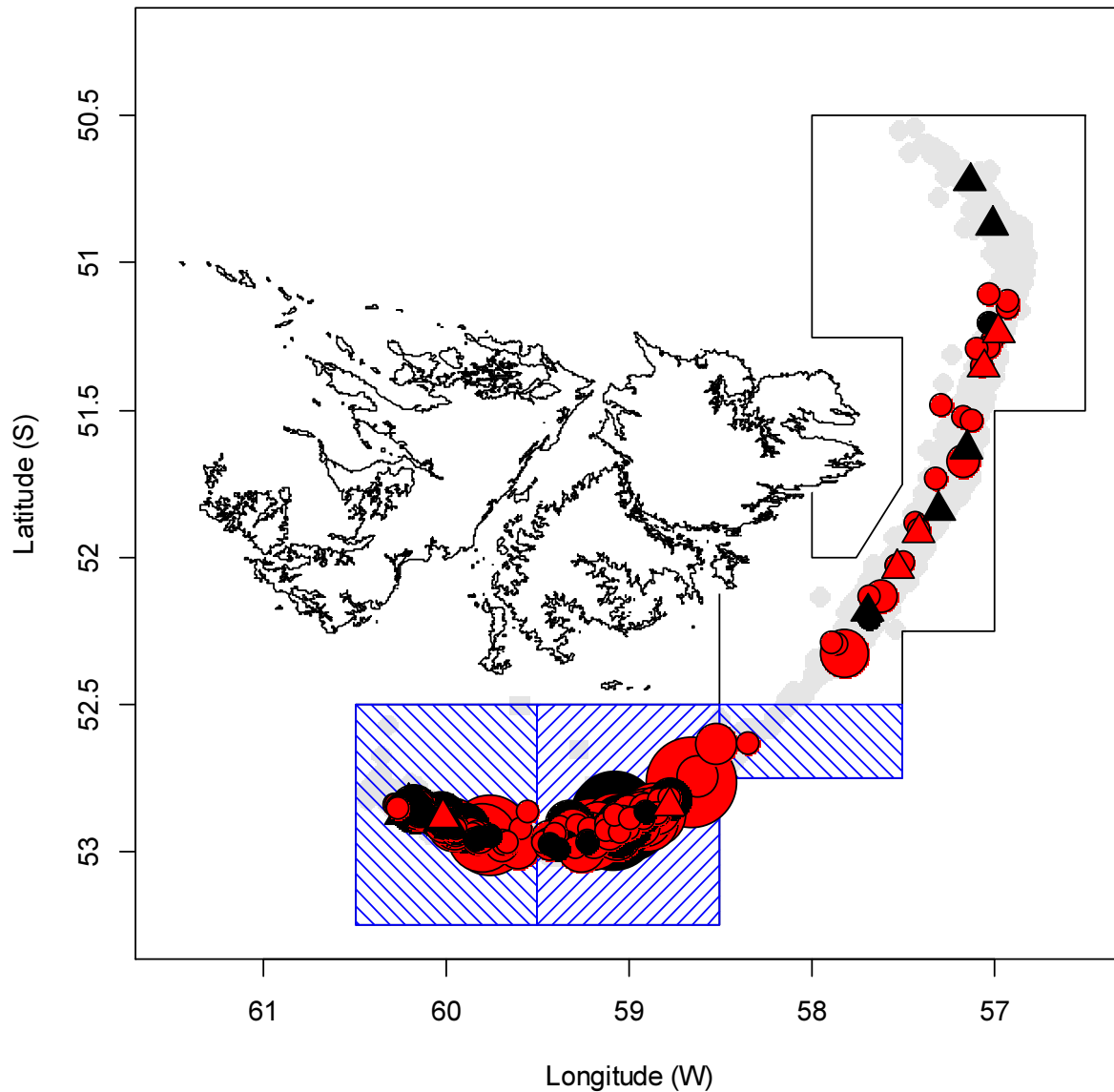
Figure 11. Distribution of trawl-caught pinnipeds during the 2nd season. Triangles: *Otaria flavescens*, circles: *Arctocephalus australis*. Black: dead animals, red: live animals. Symbols size-scaled to numbers caught per vessel-day; maximum = 14. Blue right-shaded area: initial pinniped exclusion zone. Blue left-shaded areas: additional pinniped exclusion zones. Grey under-shading: distribution of trawls, equivalent to Figure 2.

A generalized linear model (GLM) was calculated to examine if the distribution of pinniped bycatches by vessel-day could be related to variables of the fishery. Variables tested were: SED[d], number of observers on board (0, 1 or 2), observers' affiliations (FIG, ex-FIG,

---

[d] For this computation designated by the three categories 'none', 'Lobitera', or 'EuroRed'.

MRAG or CapFish)[e], latitude, longitude, depth[f] (as 3rd-degree polynomials to comprise potentially non-linear effects), chronological day, total trawl hours of the vessel-day, average hours per trawl, reported catch weight of *D. gahi*, radial distance from Beauchêne Island[g], and two clustering indices that consisted of the number of vessels within 20 km of each vessel on the same day, and the number of vessels within 20 km of the position of each vessel on the day before. The purpose of the clustering indices was to evaluate if pinnipeds were attracted to concentrations of vessels (with and without delay), or correspondingly attracted to concentrations of each other. The clustering distance of 20 km was chosen as the approximate minimum foraging range of *Arctocephalus australis* (Thompson et al. 2003). Two obvious factorial variables to be included in the GLM were the individual vessel and the individual observer. However, these were repartitioned asymmetrically throughout the season as FIG observers moved between multiple vessels whereas contracted marine mammal monitors remained assigned to one vessel. Therefore, a combined vessel / observer factorial index was implemented, consisting altogether of 50 categorical combinations (including 16 "vessel – none"). Significant variables were selected by a backward algorithm on the criterion that the variable improved deviance of the GLM by ≥1% (Starr 2012).

  The GLM was computed for fur seals and sea lions separately, as the two species did not show correlated distributions, and for dead animals only, as live capture reports were ambiguous to quantify; especially once SEDs were in use. However, dead sea lions were too infrequent to obtain interpretable results (9 total), and the following discussion is about fur seals only.

Table 2. GLM variables and deviance explained for dead fur seal captures per vessel-day. 'Percent explained' per variable was calculated by removing each variable in turn from the GLM, subtracting the deviance explained of the reduced GLM from the deviance explained of the full GLM and normalizing the differences relative to the full GLM.

Variable	Percent explained
Vessel / Observer	35.6
Distance from Beauchêne I.	11.2
Depth	9.7
N Observers	6.3
Latitude	4.2
SED	3.9
20 km cluster – day before	2.7
Total	73.5

  Seven variables were found significant and together explained 73.5% of the GLM deviance in dead fur seal captures (Table 2). Nearly half of that deviance explained was taken by the individual combination of vessel / observer, reflecting that in an "unplanned experiment" such as this season much of the outcome remains a matter of circumstance. The six descriptive variables are plotted on Figure 12. Next highest in Table 2: the distance from

---

[e] When two observers were on board it was one FIG observer plus one contracted marine mammal monitor, and FIG was taken as the senior affiliation.
[f] Latitude, longitude and depth were averaged per vessel-day by the weighted averages of trawl durations reported in the electronic logbooks.
[g] Fishery Officers deployed during the season reported sighting numerous fur seals and sea lions on Beauchêne Island, suggesting that this was their primary local haul-out (FishOps, pers. comm.).
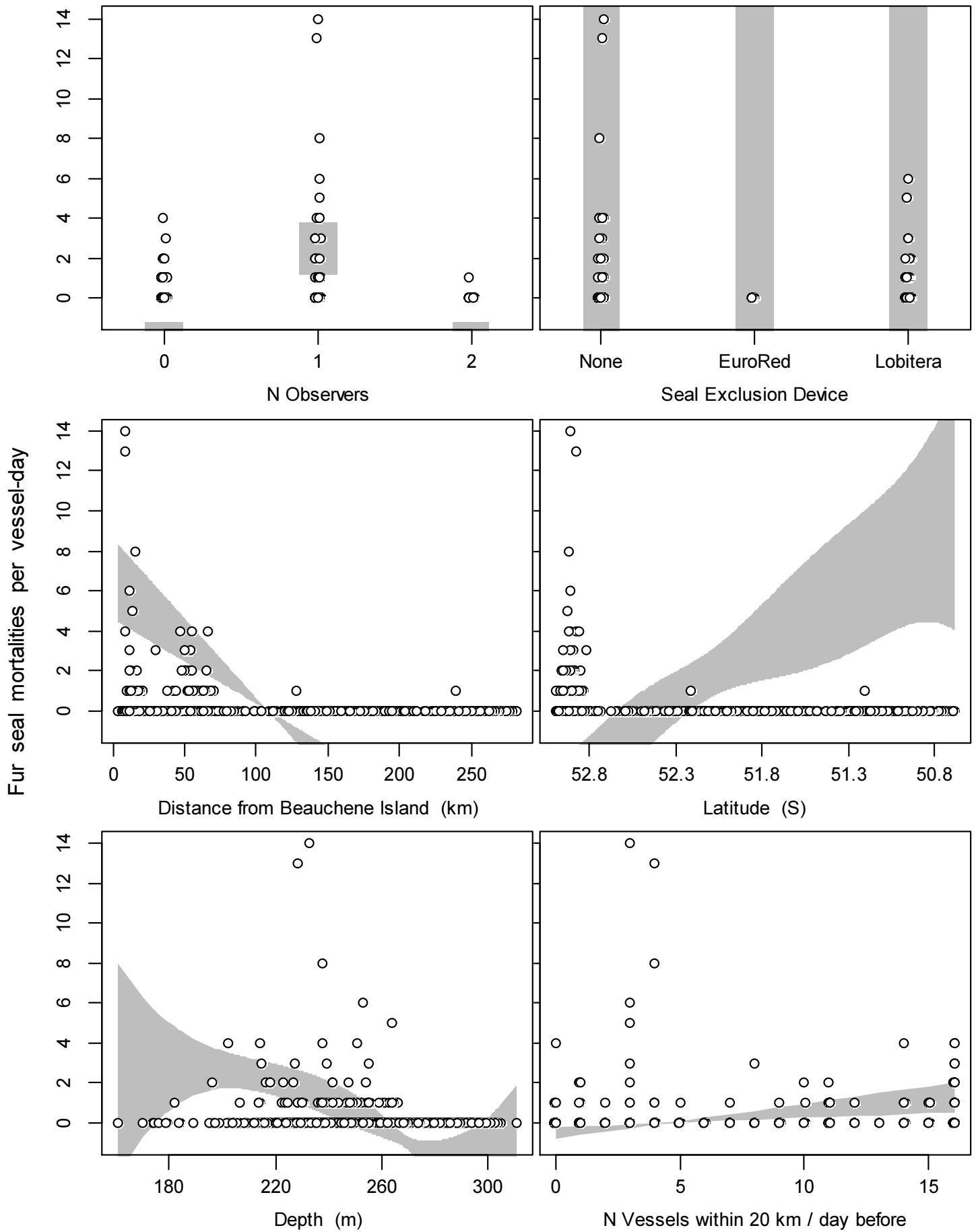
Figure 12 [previous page]. Fur seal mortalities per vessel-day vs. significant GLM explanatory variables. Grey under-shading: marginal trends of the explanatory variables ± 1.96 standard errors.

Beauchêne Island had a strongly negative correlation with fur seal bycatch, consistent with the expected distribution of pinnipeds as central-place foragers (Womble et al. 2009) and observations in other fisheries (Hamer and Goldsworthy 2006). Depth had a somewhat dome-shaped correlation with fur seal bycatch, indicative that attendance of fur seals corresponded to the preferred fishing depths. Fur seal bycatches were significantly higher with 1 observer than zero observers, suggesting stricter reporting, but not higher with 2 observers, which may be an artefact as two observers were relatively infrequent and predominantly in the latter part of the season when fur seal bycatches had decreased. If observer numbers were classified as present / absent instead of 0, 1, 2 in the GLM, fur seal bycatches also had a significantly positive correlation with observer presence (data not shown). Latitude had a northward-positive correlation with fur seal bycatch. This appears counter-intuitive (Figure 12), as the fur seal bycatches were clearly concentrated south. However, the main axis of distance from Beauchêne Island was already north-south, so latitude represented a residual effect relative to the extent that vessels were not unequally far away from Beauchêne Island. SEDs added significant explanatory power to the total GLM, but variation was high in all three categories (none, EuroRed, Lobitera) as most (>85%) vessel-days reported no dead fur seals irrespective of their SED status. Finally, fur seal mortalities had a small but significant positive correlation with the number of vessels clustered around a given vessel the day before, suggesting that fur seals behave aggregately in feeding around fishing trawlers, but take some time to catch up.

Overall, the GLM pointed to proximate location with the fishery as the most identifiable cause of the high level of pinniped bycatches. Chronological day was not retained as a significant variable, discounting the hypothesis that pinniped abundance in this season might just have been an unusually (and unluckily) timed event. One notable observation is that either species – South American fur seal or Southern sea lion – alone would have represented exceptionally high bycatch, whereby the two species did not appear to interact with each other in the *D. gahi* fishing zone. The continuing pattern of pinniped distributions will need to be monitored throughout forthcoming seasons.

Fishery bycatch

Of the 1002 2nd season vessel-days (Table 1), five vessel-days reported a primary catch other than *D. gahi*: one vessel-day reported 61.7% rock cod (*Patagonotothen ramsayi*) vs. 38.3% *D. gahi*; four vessel-days reported 44.1%, 68.9%, 57.3% and 57.3% blue whiting (*Micromesistius australis*) vs. 41.5%, 29.3%, 41.3% and 39.0% *D. gahi*. The one catch report with primary rock cod occurred on August 9th; the four catch reports with primary blue whiting occurred later in the season between September 23rd and 2nd October.

The most common total bycatches reported for the 2nd season 2017 were rock cod (1130 t, reported from 997 vessel-days), blue whiting (299 t, 312 vessel-days), skate (Rajidae) (98 t, 627 vessel-days), red cod (*Salilota australis*) (71 t, 328 vessel-days), common hake (*Merluccius hubbsi*) (61 t, 469 vessel-days), hoki (*Macruronus magellanicus*), (50 t, 113 vessel-days), grenadier (*Macrourus* spp.) (36 t, 308 vessel-days), and lobster krill (*Munida* spp.) (31 t, 89 vessel-days). Relative distributions by grid of these bycatches are shown in Figure 13, and the complete list of all catches by species or species group is given in Table A1.
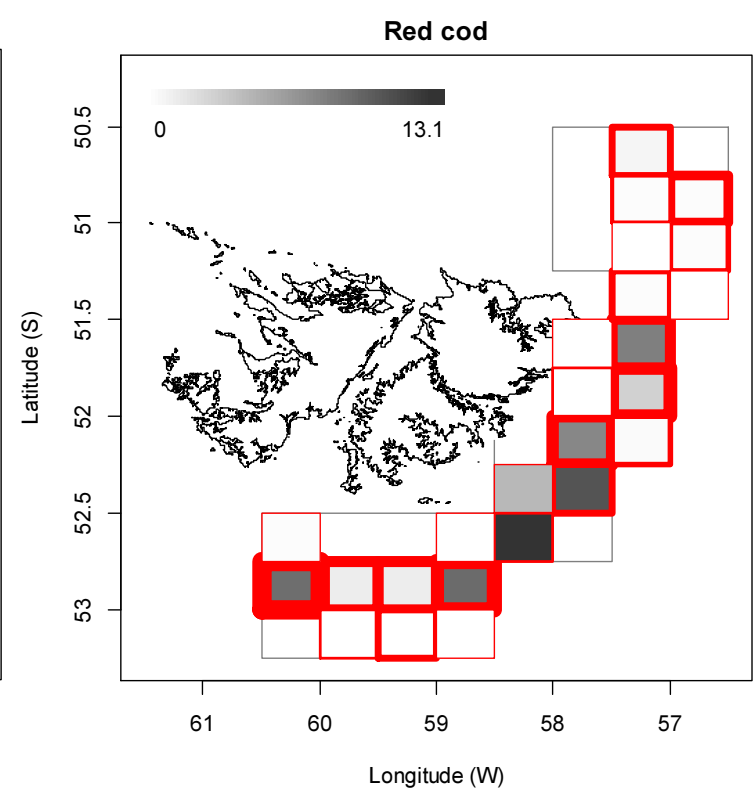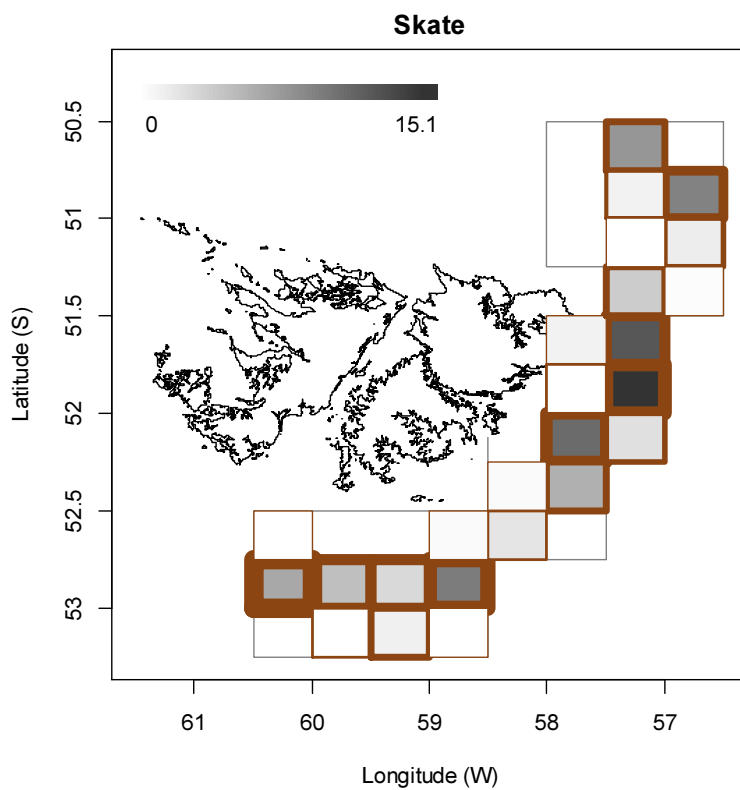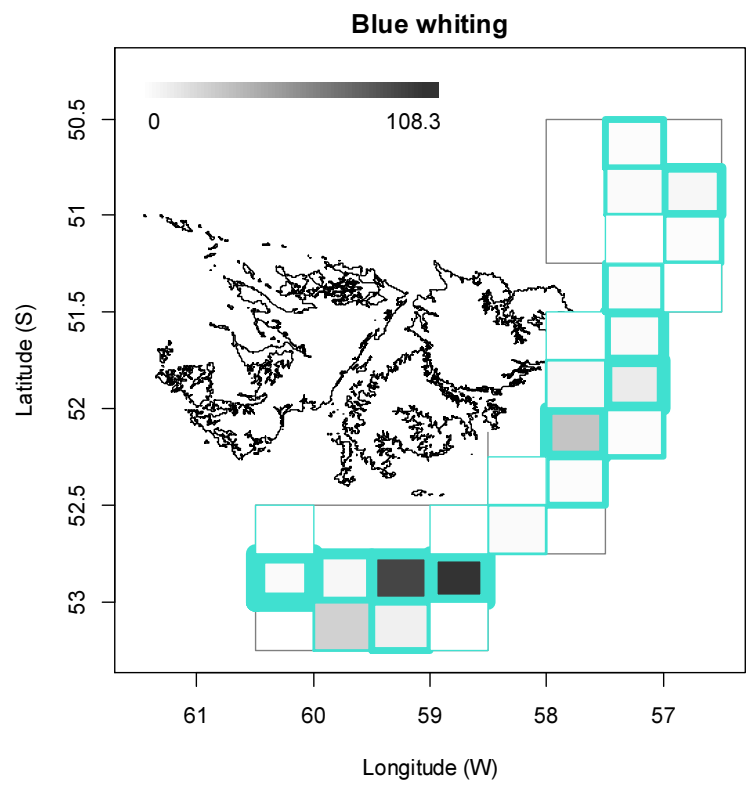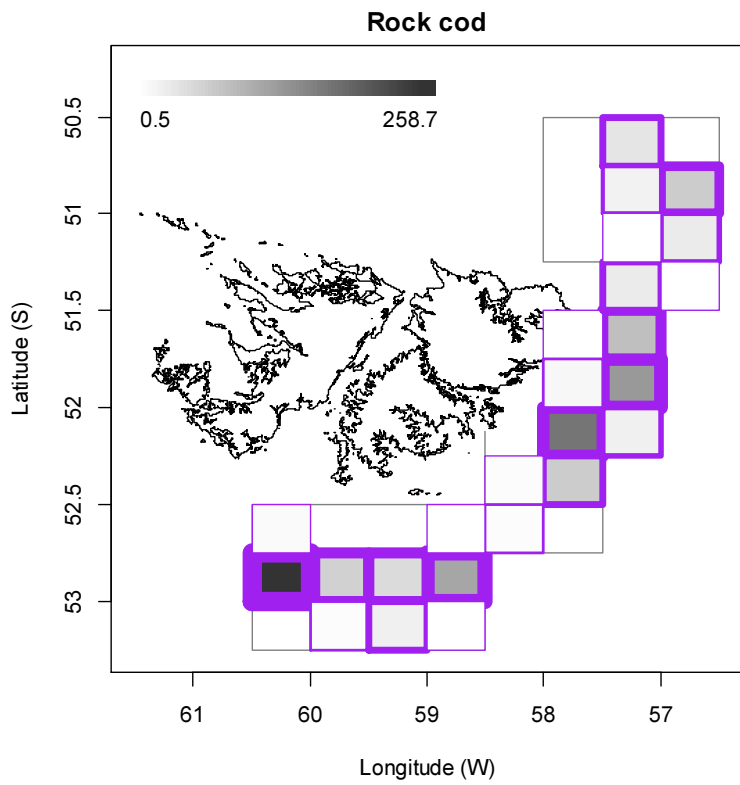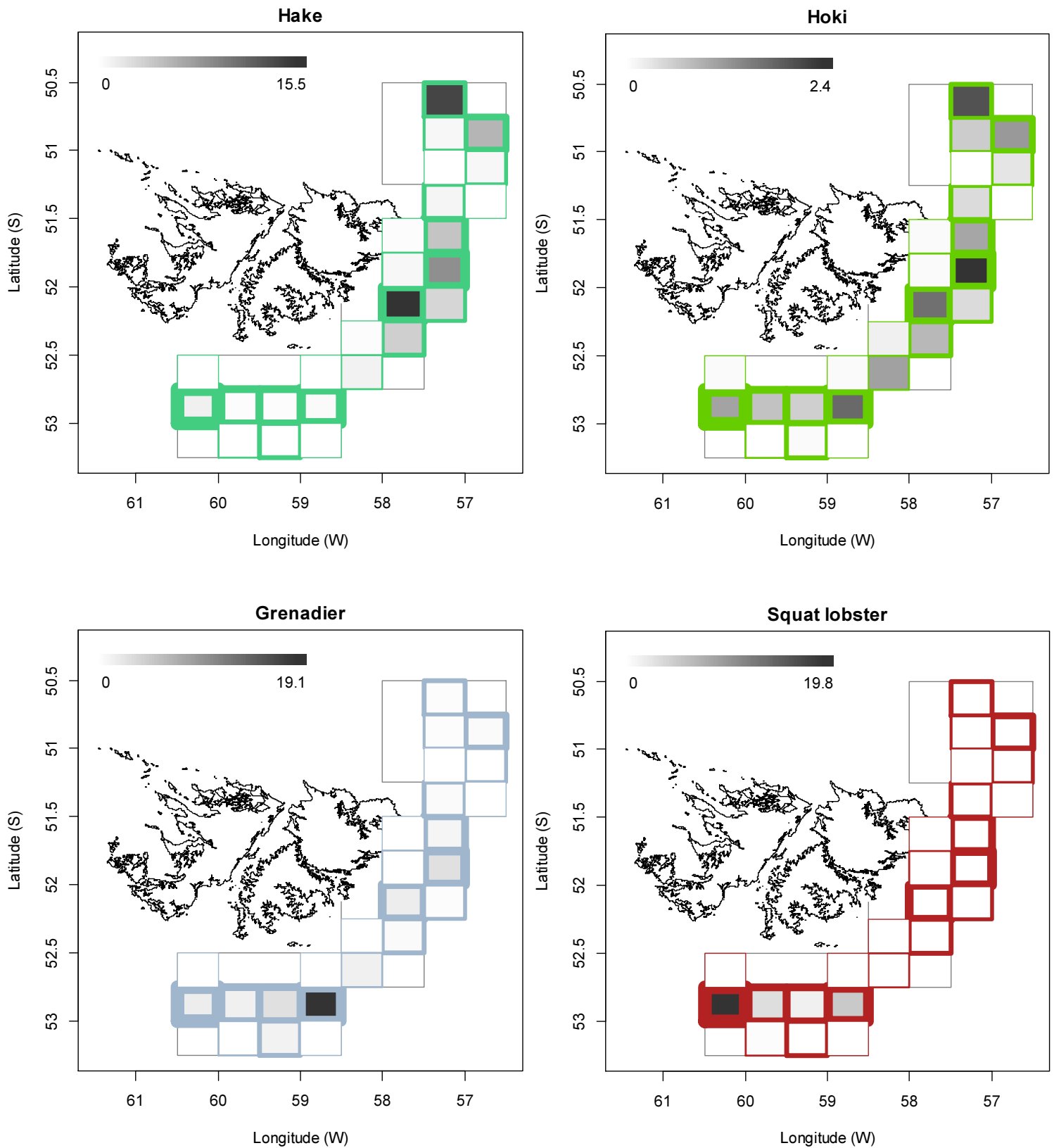
Figure 13. Distributions of the eight principal bycatches during *D. gahi* 2nd season 2017, by noon position grids. Thickness of grid lines is proportional to the number of vessel-days (1 to 206 per grid; 25 different grids were occupied). Gray-scale is proportional to the bycatch biomass; maximum (tonnes) indicated on each plot.

References

Agnew, D.J., Baranowski, R., Beddington, J.R., des Clers, S., Nolan, C.P. 1998. Approaches to assessing stocks of *Loligo gahi* around the Falkland Islands. Fisheries Research 35: 155-169.

Agnew, D. J., Beddington, J. R., and Hill, S. 2002. The potential use of environmental information to manage squid stocks. Canadian Journal of Fisheries and Aquatic Sciences, 59: 1851–1857.

Arkhipkin, A. 1993. Statolith microstructure and maximum age of *Loligo gahi* (Myopsida: Loliginidae) on the Patagonian Shelf. Journal of the Marine Biological Association of the UK 73: 979-982.

Arkhipkin, A.I., Middleton, D.A.J. 2002. Sexual segregation in ontogenetic migrations by the squid *Loligo gahi* around the Falkland Islands. Bulletin of Marine Science 71: 109-127.

Arkhipkin, A.I., Middleton, D.A.J., Barton, J. 2008. Management and conservation of a short-lived fishery resource: *Loligo gahi* around the Falkland Islands. American Fisheries Society Symposium 49: 1243-1252.

Barton, J. 2002. Fisheries and fisheries management in Falkland Islands Conservation Zones. Aquatic Conservation: Marine and Freshwater Ecosystems 12: 127–135.

Blake, D. 2017. Observer Report 1153. Technical Document, FIG Fisheries Department. 15 p.

Boag, T. 2017a. Observer Report 1149. Technical Document, FIG Fisheries Department. 24 p.

Boag, T. 2017b. Observer Report 1154. Technical Document, FIG Fisheries Department. 31 p.

Boag, T. 2017c. Observer Report 1155. Technical Document, FIG Fisheries Department. 31 p.

Brooks, S.P., Gelman, A. 1998. General methods for monitoring convergence of iterative simulations. Journal of computational and graphical statistics 7:434-455.

Chen, X., Chen, Y., Tian, S., Liu, B., Qian, W. 2008. An assessment of the west winter-spring cohort of neon flying squid (*Ommastrephes bartramii*) in the Northwest Pacific Ocean. Fisheries Research 92: 221-230.

DeLury, D.B. 1947. On the estimation of biological populations. Biometrics 3: 145-167.

Derbyshire, C. 2017a. Observer Report 1151. Technical Document, FIG Fisheries Department. 21 p.

Derbyshire, C. 2017b. Observer Report 1152. Technical Document, FIG Fisheries Department. 25 p.

Derbyshire, C. 2017c. Observer Report 1166. Technical Document, FIG Fisheries Department. 45 p.

Derbyshire, C. 2017d. Observer Report 1167. Technical Document, FIG Fisheries Department. 31 p.

Gamerman, D., Lopes, H.F. 2006. Markov Chain Monte Carlo. Stochastic simulation for Bayesian inference. 2nd edition. Chapman & Hall/CRC.

Hamer, D.J., Goldsworthy, S.D. 2006. Seal-fishery operational interactions: Identifying the environmental and operational aspects of a trawl fishery that contribute to by-catch and mortality of Australian fur seals (*Arctocephalus pusillus doriferus*). Biological Conservation 130: 517-529.

Hamilton, S., Baker, G.B. 2015. Review of research and assessments on the efficacy of sea lion exclusion devices in reducing the incidental mortality of New Zealand sea lions *Phocarctos hookeri* in the Auckland Islands squid trawl fishery. Fisheries Research 161: 200-206.

Hoenig, J.M. 1983. Empirical use of longevity data to estimate mortality rates. Fishery Bulletin 82: 898-903.

Huillier, J.-T. 2017a. Observer Report 1150. Technical Document, FIG Fisheries Department. 19 p.

Huillier, J.-T. 2017b. Observer Report 1158. Technical Document, FIG Fisheries Department. 21 p.

Huillier, J.-T. 2017c. Observer Report 1159. Technical Document, FIG Fisheries Department. 16 p.

Huillier, J.-T. 2017d. Observer Report 1160. Technical Document, FIG Fisheries Department. 14 p.

Huillier, J.-T. 2017e. Observer Report 1161. Technical Document, FIG Fisheries Department. 20 p.

Iriarte, V. 2017a. Observer Report 1156. Technical Document, FIG Fisheries Department. 17 p.

Iriarte, V. 2017b. Observer Report 1157. Technical Document, FIG Fisheries Department. 27 p.

Iriarte, V. 2017c. Observer Report 1162. Technical Document, FIG Fisheries Department. 12 p.

Iriarte, V. 2017d. Observer Report 1163. Technical Document, FIG Fisheries Department. 14 p.

Jacobson, L.D., Cadrin, S.X., Weinberg, J.R. 2002. Tools for estimating surplus production and F_{MSY} in any stock assessment model. North American Journal of Fisheries Management 22: 326-338.

Keller, S., Robin, J.P., Valls, M., Gras, M., Cabanellas-Reboredo, M., Quetglas, A. 2015. The use of depletion models to assess Mediterranean cephalopod stocks under the current EU data collection framework. Mediterranean Marine Science 16: 513-523.

Magnusson, A., Punt, A., Hilborn, R. 2013. Measuring uncertainty in fisheries stock assessment: the delta method, bootstrap, and MCMC. Fish and Fisheries 14: 325-342.

Medellín-Ortiz, A., Cadena-Cárdenas, L., Santana-Morales, O. 2016. Environmental effects on the jumbo squid fishery along Baja California's west coast. Fisheries Science 82: 851-861.

Mercopress. 2017a. http://en.mercopress.com/2017/08/11/falklands-second-loligo-season-very-promising-but-by-catch-of-fur-seals-forces-an-exclusion-zone

Mercopress. 2017b. http://en.mercopress.com/2017/08/18/falklands-outwitting-canny-fur-seals-feasting-on-abundant-loligo.

Morales-Bojórquez, E., Hernández-Herrera, A., Cisneros-Mata, M.A., Nevárez-Martínez, M.O. 2008. Improving estimates of recruitment and catchability of jumbo squid *Dosidicus gigas* in the Gulf of California, Mexico. Journal of Shellfish Research 27: 1233-1237.

Mueter, F.J., Megrey, B.A. 2006. Using multi-species surplus production models to estimate ecosystem-level maximum sustainable yields. Fisheries Research 81: 189-201.

Nash, J.C., Varadhan, R. 2011. optimx: A replacement and extension of the optim() function. R package version 2011-2.27. http://CRAN.R-project.org/package=optimx

Patterson, K.R. 1988. Life history of Patagonian squid *Loligo gahi* and growth parameter estimates using least-squares fits to linear and von Bertalanffy models. Marine Ecology Progress Series 47: 65-74.

Payá, I. 2010. Fishery Report. *Loligo gahi*, Second Season 2009. Fishery statistics, biological trends, stock assessment and risk analysis. Technical Document, Falkland Islands Fisheries Dept. 54 p.

Pierce, G.J., Guerra, A. 1994. Stock assessment methods used for cephalopod fisheries. Fisheries Research 21: 255 – 285.

Punt, A.E., Hilborn, R. 1997. Fisheries stock assessment and decision analysis: the Bayesian approach. Reviews in Fish Biology and Fisheries 7:35-63.

Roa-Ureta, R. 2012. Modelling in-season pulses of recruitment and hyperstability-hyperdepletion in the *Loligo gahi* fishery around the Falkland Islands with generalized depletion models. ICES Journal of Marine Science 69: 1403–1415.

Roa-Ureta, R., Arkhipkin, A.I. 2007. Short-term stock assessment of *Loligo gahi* at the Falkland Islands: sequential use of stochastic biomass projection and stock depletion models. ICES Journal of Marine Science 64: 3-17.

Rosenberg, A.A., Kirkwood, G.P., Crombie, J.A., Beddington, J.R. 1990. The assessment of stocks of annual squid species. Fisheries Research 8: 335-350.

Royer, J., Périès, P., Robin, J.P. 2002. Stock assessments of English Channel loliginid squids: updated depletion methods and new analytical methods. ICES Journal of Marine Science 59: 445-457.

Shaw, P.W., Arkhipkin, A.I., Adcock, G.J., Burnett, W.J., Carvalho, G.R., Scherbich, J.N., Villegas, P.A. 2004. DNA markers indicate that distinct spawning cohorts and aggregations of Patagonian squid, *Loligo gahi*, do not represent genetically discrete subpopulations. Marine Biology, 144: 961-970.

Starr, P.J. 2012. Standardised CPUE analysis exploration: using the rock lobster voluntary logbook and observer catch sampling programmes. New Zealand Fisheries Assessment Report 2012/34. Ministry for Primary Industries, 75 p.

Swartzman, G., Huang, C., Kaluzny, S. 1992. Spatial analysis of Bering Sea groundfish survey data using generalized additive models. Canadian Journal of Fisheries and Aquatic Sciences 49: 1366-1378.

Thompson, D., Moss, S.E.W., Lovell, P. 2003. Foraging behaviour of South American fur seals *Arctocephalus australis*: extracting fine scale foraging behaviour from satellite tracks. Marine Ecology Progress Series 260: 285-296.

Winter, A. 2014. *Loligo* stock assessment, second season 2014. Technical Document, Falkland Islands Fisheries Department. 30 p.

Winter, A. 2016. Falkland calamari stock assessment, second season 2016. Technical Document, Falkland Islands Fisheries Department. 28 p.

Winter, A. 2017. Stock assessment – Falkland calamari (*Doryteuthis gahi*). Technical Document, Falkland Islands Fisheries Department. 30 p.

Winter, A., Arkhipkin, A. 2015. Environmental impacts on recruitment migrations of Patagonian longfin squid (*Doryteuthis gahi*) in the Falkland Islands with reference to stock assessment. Fisheries Research 172: 85-95.

Winter, A., Shcherbich, Z., Iriarte, V. Derbyshire, C. 2017. *Doryteuthis gahi* stock assessment survey, 2nd season 2017. Technical Document, Falkland Islands Fisheries Department. 25 p.

Womble, J.N., Sigler, M.F., Willson, M.F. 2009. Linking seasonal distribution patterns with prey availability in a central-place forager, the Steller sea lion. Journal of Biogeography 36: 439-451.

Young, I.A.G., Pierce, G.J., Daly, H.I., Santos, M.B., Key, L.N., Bailey, N., Robin, J.-P., Bishop, A.J., Stowasser, G., Nyegaard, M., Cho, S.K., Rasero, M., Pereira, J.M.F. 2004. Application of depletion methods to estimate stock size in the squid *Loligo forbesi* in Scottish waters (UK). Fisheries Research 69: 211-227.

Zhang, H.-M., Bates, J.J., Reynolds, R.W. 2006. Assessment of composite global sampling: Sea surface wind speed. Geophysical Research Letters 33: L17714.

Appendix
Doryteuthis gahi individual weights
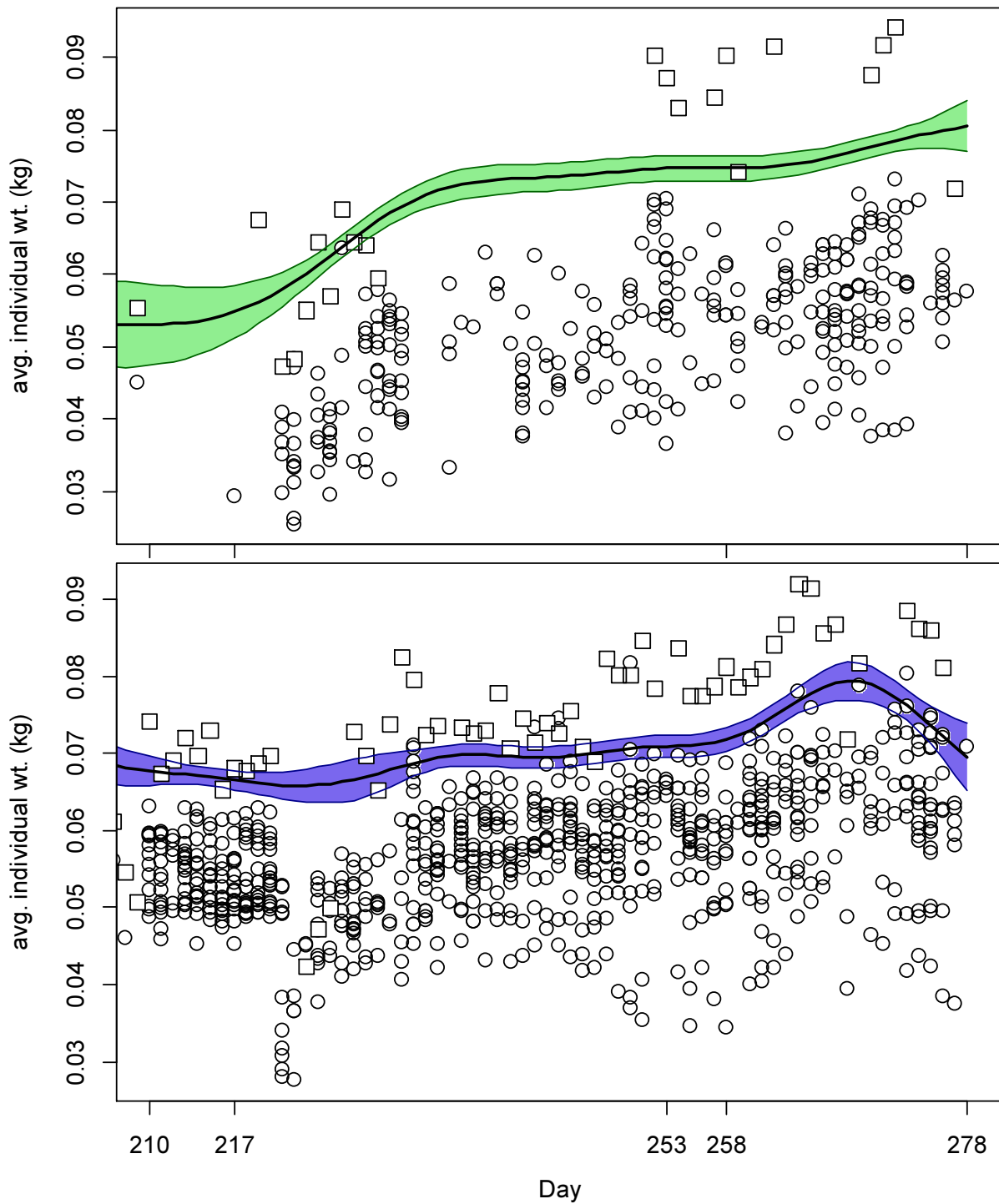
Figure A1. North (top) and south (bottom) sub-area daily average individual *D. gahi* weights from commercial size categories per vessel (circles) and observer measurements (squares). GAMs of the daily trends ± 95% confidence intervals (centre lines and colour under-shading).

To smooth fluctuations, generalized additive model (GAM) trends were calculated of daily average individual weights. North and south sub-areas were calculated separately. For

continuity, the GAMs were calculated using all pre-season survey and in-season data contiguously. North and south GAMs were first calculated separately on the commercial and observer data. The commercial data GAMs were taken as the baseline trends, and calibrated to the observer data GAMs in proportion to the correlation between the commercial data and observer data GAMs. For example, if the season average individual weight estimate from commercial data was 0.052 kg, the season average individual weight estimate from observer data was 0.060 kg, and the coefficient of determination (R^2) between commercial and observer GAM trends was 86%, then the resulting trend of daily average individual weights was calculated as the commercial data GAM values + (0.060 − 0.052) × 0.86. This way, both the greater day-to-day consistency of the commercial data trends, and the greater point value accuracy of the observer data are represented in the calculations. GAM plots of the north and south sub-areas are shown in Figure A1.

Prior estimates and CV

The pre-season survey (Winter et al., 2017) had estimated *D. gahi* biomasses of 17,693 t (standard deviation: ± 2,486 t) north of 52.5° S and 39,115 t (standard deviation: 5,428 t) south of 52.5° S[h]. From modelled survey catchability, Payá (2010) had estimated average net escapement of up to 22%, which was added to the standard deviation:

$$39,115 \pm \left(\frac{5,428}{39,115} + .22 \right) \; = \; 39,115 \pm 35.9\% \qquad = \; 39,115 \pm 14,033 \text{ t} \qquad \textbf{(A1-S)}$$

$$17,693 \pm \left(\frac{2,486}{17,693} + .22 \right) \; = \; 17,693 \pm 36.1\% \qquad = \; 17,693 \pm 6,379 \text{ t} \qquad \textbf{(A1-N)}$$

The 22% was added as a linear increase in the variability, but was not used to reduce the total estimate, because squid that escape one trawl are likely to be part of the biomass concentration that is available to the next trawl.

   D. gahi numbers at the end of the survey were estimated as the survey biomasses divided by the GAM-predicted individual weight averages for the survey: 0.0536 kg north, 0.0698 kg south (Figure A1), and 0.0655 kg combined. Average coefficients of variation (CV) of the GAM over the duration of the pre-season survey were 5.7% north and 2.8% south; and CV of the length-weight conversion relationship (Equation **8**) were 6.6% north and 6.9% south. Combining these sources of variation with the pre-season survey biomass estimates and individual weight averages (above) gave estimated *D. gahi* numbers at survey end (day 209) of:

$$\text{prior } N_{S \text{ day } 209} \; = \; \frac{39,115 \times 1000}{0.0698} \pm \sqrt{35.9\%^2 + 2.8\%^2 + 6.9^2}$$

$$= \; 0.560 \times 10^9 \pm 36.6\%$$

$$\text{prior } N_{N \text{ day } 209} \; = \; \frac{17,693 \times 1000}{0.0536} \pm \sqrt{36.1\%^2 + 5.7\%^2 + 6.6\%^2}$$

---

[h] Note that these are not the north and south values quoted in Winter et al. (2017), because the delineation between north and south was not switched from 52°S to 52.5°S latitude until after the pre-season survey.

$$= 0.330 \times 10^9 \pm 37.1\%$$

Priors were normalized for the combined fishing zone average, to produce better continuity as vessels fish sometimes north and sometimes south:

$$_{\text{nprior}} N_{\text{S day 209}} = \left(\frac{(39{,}115 + 17{,}693) \times 1000}{0.0655} \right) \times \left(\frac{_{\text{prior}} N_{\text{S day 209}}}{_{\text{prior}} N_{\text{N day 209}} + _{\text{prior}} N_{\text{S day 209}}} \right)$$

$$= 0.546 \times 10^9 \pm 36.6\% \qquad \textbf{(A2-S)}$$

$$_{\text{nprior}} N_{\text{N day 209}} = \left(\frac{(17{,}693 + 39{,}115) \times 1000}{0.0655} \right) \times \left(\frac{_{\text{prior}} N_{\text{N day 209}}}{_{\text{prior}} N_{\text{N day 209}} + _{\text{prior}} N_{\text{S day 209}}} \right)$$

$$= 0.321 \times 10^9 \pm 37.1\% \qquad \textbf{(A2-N)}$$

The catchability coefficient (q) prior for the south sub-area was taken on day 210, the first day of the season, when all 12 vessels that entered the fishery that day proceeded south. Abundance was discounted for one day's mortality as the survey had ended the day before:

$$_{\text{nprior}} N_{\text{S day 210}} = {}_{\text{nprior}} N_{\text{S day 209}} \times e^{-M \cdot (210 - 209)} - CNMD_{\text{day 210}} = 0.538 \times 10^9 \quad \textbf{(A3-S)}$$

where $CNMD_{\text{day 58}} = 0$ as no catches intervened between the end of the survey and the start of commercial season. Thus:

$$_{\text{prior}} q_{\text{S}} = C(N)_{\text{S day 210}} / (_{\text{nprior}} N_{\text{S day 210}} \times E_{\text{S day 210}})$$

$$= (C(B)_{\text{S day 210}} / Wt_{\text{S day 210}}) / (_{\text{nprior}} N_{\text{S day 210}} \times E_{\text{S day 210}})$$

$$= (723.9 \text{ t} / 0.0677 \text{ kg}) / (0.538 \times 10^9 \times 12 \text{ vessel-days})$$

$$= 1.655 \times 10^{-3} \text{ vessels}^{-1 \text{ i}} \qquad \textbf{(A4-S)}$$

CV of the prior was calculated as the sum of variability in $_{\text{nprior}} N_{\text{S day 209}}$ (Equations **A2-S**) plus variability in the catches of vessels on start day 210, plus variability of the natural mortality (see Appendix section Natural mortality, below):

$$CV_{\text{prior S}} = \sqrt{36.6\%^2 + \left(\frac{SD\left(C(B)_{\text{S vessels day 210}}\right)}{\text{mean}\left(C(B)_{\text{S vessels day 210}}\right)} \right)^2 + \left(1 - \text{sign}(1 - CV_M) \times \text{abs}(1 - CV_M)^{(210-209)}\right)^2}$$

$$= \sqrt{36.6\%^2 + 23.2\%^2 + 15.5\%^2} = 46.0\% \qquad \textbf{(A5-S)}$$

The catchability coefficient (q) prior for the north sub-area was calculated on day 217, when one vessel first fished north and the initial depletion period north started. Abundance on day 217 was discounted for natural mortality over the days since the end of the survey:

$$_{\text{nprior}} N_{\text{N day 217}} = {}_{\text{nprior}} N_{\text{N day 209}} \times e^{-M \cdot (217 - 209)} - CNMD_{\text{day 217}} = 0.289 \times 10^9 \quad \textbf{(A3-N)}$$

---

i On Figure 6-left.

where CNMD $_{\text{day 217}}$ = 0 as no catches had been taken between day 209 and day 217. Thus:

$$_{\text{prior}} q_N = C(N)_{N \text{ day 217}} / (_{\text{nprior}} N_{N \text{ day 217}} \times E_{N \text{ day 217}})$$

$$= (C(B)_{N \text{ day 217}} / Wt_{N \text{ day 217}}) / (_{\text{nprior}} N_{N \text{ day 217}} \times E_{N \text{ day 217}})$$

$$= (14.6 \text{ t} / 0.0548 \text{ kg}) / (0.289 \times 10^9 \times 1 \text{ vessel-day})$$

$$= 0.922 \times 10^{-3} \text{ vessels}^{-1 \text{ j}} \tag{A4-N}$$

CV of the prior was calculated as the sum of variability in $_{\text{nprior}} N_{N \text{ day 209}}$ (Equations **A2-N**) plus variability in the vessel catch on start day 217, plus variability of the natural mortality:

$$CV_{\text{prior N}} = \sqrt{37.1\%^2 + \left(\frac{SD\left(C(B)_{N \text{ vessels day 217}}\right)}{\text{mean}\left(C(B)_{N \text{ vessels day 217}}\right)} \right)^2 + \left(1 - \text{sign}(1 - CV_M) \times \text{abs}(1 - CV_M)^{(217-209)}\right)^2}$$

$$= \sqrt{37.1\%^2 + 0\%^2 + 73.9\%^2} \quad = 82.7\% \tag{A5-N}$$

Note that natural mortality variability is high because of the long delay before the first day of commercial fishing, but vessel catch variability is zero because only one vessel fished that first day. This may seem artefactual, but the ostensible absence of uncertainty by starting the depletion model on one single vessel fishing is offset by greater uncertainty within the depletion model itself.

Depletion model estimates and CV

For the south sub-area, the equivalent of Equation **3** with two N $_{\text{day}}$ was optimized on the difference between predicted catches and actual catches (Equation **4**), resulting in parameters values:

$$_{\text{depletion}} N1_{S \text{ day 210}} = 0.469 \times 10^9; \qquad _{\text{depletion}} N2_{S \text{ day 253}} = 0.088 \times 10^9$$

$$_{\text{depletion}} q_{S \text{ NSED}} = 2.220 \times 10^{-3 \text{ k}}$$

$$_{\text{depletion}} q_{S \text{ SED}} = 1.757 \times 10^{-3} \tag{A6-S}$$

The normalized root-mean-square deviation of predicted vs. actual catches was calculated as the CV of the model:

$$CV_{\text{rmsd S}} = \frac{\sqrt{\sum_{i=1}^{n} \left(_{\text{predicted}} C(N)_{S \text{ day i}} - _{\text{actual}} C(N)_{S \text{ day i}}\right)^2 / n}}{\text{mean}\left(_{\text{actual}} C(N)_{S \text{ day i}}\right)}$$

$$= 1.538 \times 10^6 / 3.134 \times 10^6 = 49.1\% \tag{A7-S}$$

---

[j] On Figure 8-left.
[k] On Figure 6-left.

$CV_{rmsd\,S}$ was added to the variability of the GAM-predicted individual weight averages for the season (Figure A1-S); equal to a CV of 1.2% south. CVs of the depletion were then calculated as the sum:

$$CV_{depletion\,S} \quad = \sqrt{CV_{rmsd\,S}{}^2 + CV_{GAM\,Wt\,S}{}^2} \quad = \sqrt{49.1\%^2 + 1.2\%^2}$$

$$= \quad 49.1\% \qquad \qquad \textbf{(A8-S)}$$

For the north sub-area, the equivalent of Equation **3** with two N_{day} was optimized on the difference between predicted catches and actual catches (Equation **4**), resulting in parameters values:

depletion $N1_{N\,day\,217}$ $\quad = 0.288 \times 10^9;$ $\qquad$ depletion $N2_{N\,day\,258}$ $\quad = 0.101 \times 10^9$

depletion $q_{N\,NSED}$ $\quad = 0.780 \times 10^{-3}$ [1]

depletion $q_{N\,SED}$ $\quad = 1.189 \times 10^{-3}$ $\qquad\qquad\qquad\qquad\qquad$ **(A6-N)**

The root-mean-square deviation of predicted vs. actual catches was calculated as the CV of the model:

$$CV_{rmsd\,N} \quad = \quad \frac{\sqrt{\sum_{i=1}^{n}\left({}_{predicted}C(N)_{N\,day\,i} - {}_{actual}C(N)_{N\,day\,i}\right)^2 / n}}{mean\left({}_{actual}C(N)_{N\,day\,i}\right)}$$

$$= \quad 0.570 \times 10^6 / 1.313 \times 10^6 \quad = \quad 43.4\% \qquad \textbf{(A7-N)}$$

$CV_{rmsd\,N}$ was added to the variability of the GAM-predicted individual weight averages for the season (Figure A1-N); equal to a CV of 1.3% north. CVs of the depletion were then calculated as the sum:

$$CV_{depletion\,N} \quad = \sqrt{CV_{rmsd\,N}{}^2 + CV_{GAM\,Wt\,N}{}^2} \quad = \sqrt{43.4\%^2 + 1.3\%^2}$$

$$= \quad 43.5\% \qquad \qquad \textbf{(A8-N)}$$

Combined Bayesian models

For the south sub-area, the joint optimization of Equations **4** and **5** resulted in parameters values:

Bayesian $N1_{S\,day\,210}$ $\quad = 0.592 \times 10^9;$ $\qquad$ Bayesian $N2_{S\,day\,253}$ $\quad = 0.101 \times 10^9$

Bayesian $q_{S\,NSED}$ $\quad = 1.671 \times 10^{-3}$ [m]

Bayesian $q_{S\,SED}$ $\quad = 1.217 \times 10^{-3}$ $\qquad\qquad\qquad\qquad\qquad$ **(A9-S)**

These parameters produced the fit between predicted catches and actual catches shown in Figure A2-S.

---

[1] On Figure 8-left.
[m] On Figure 6-left.
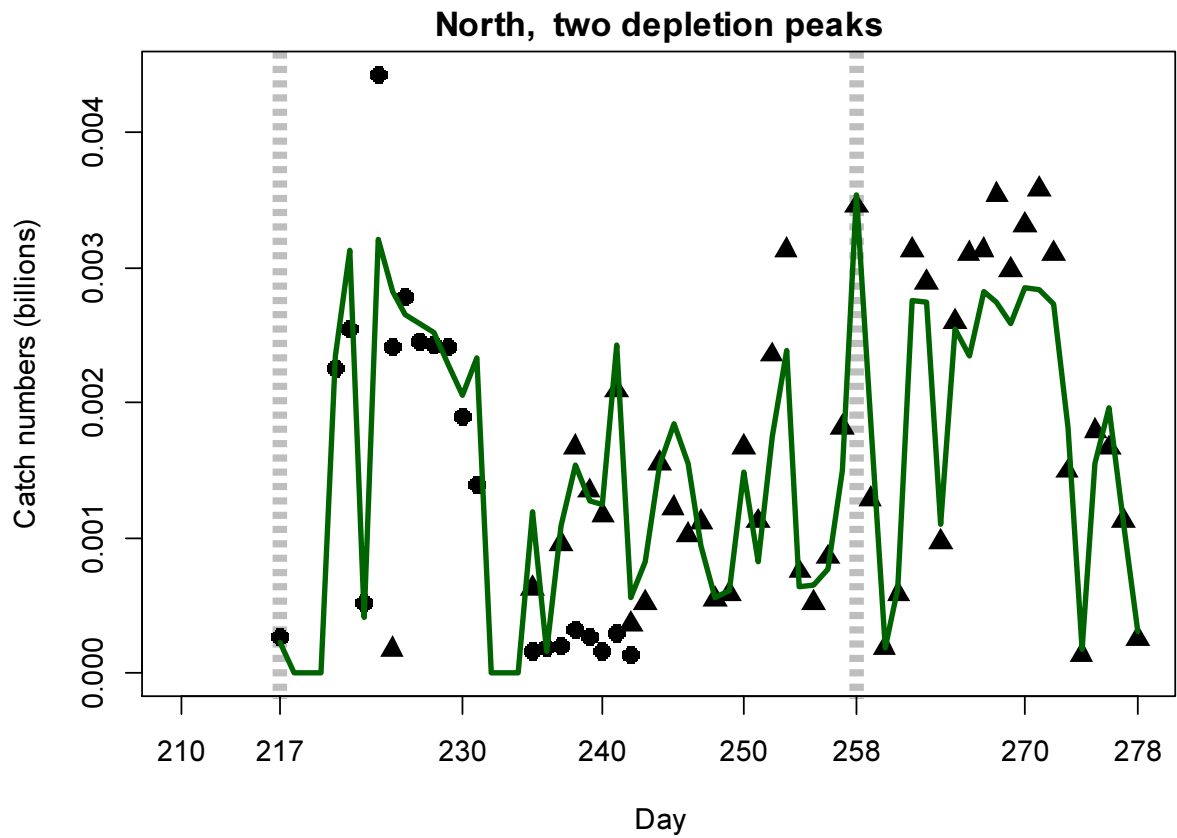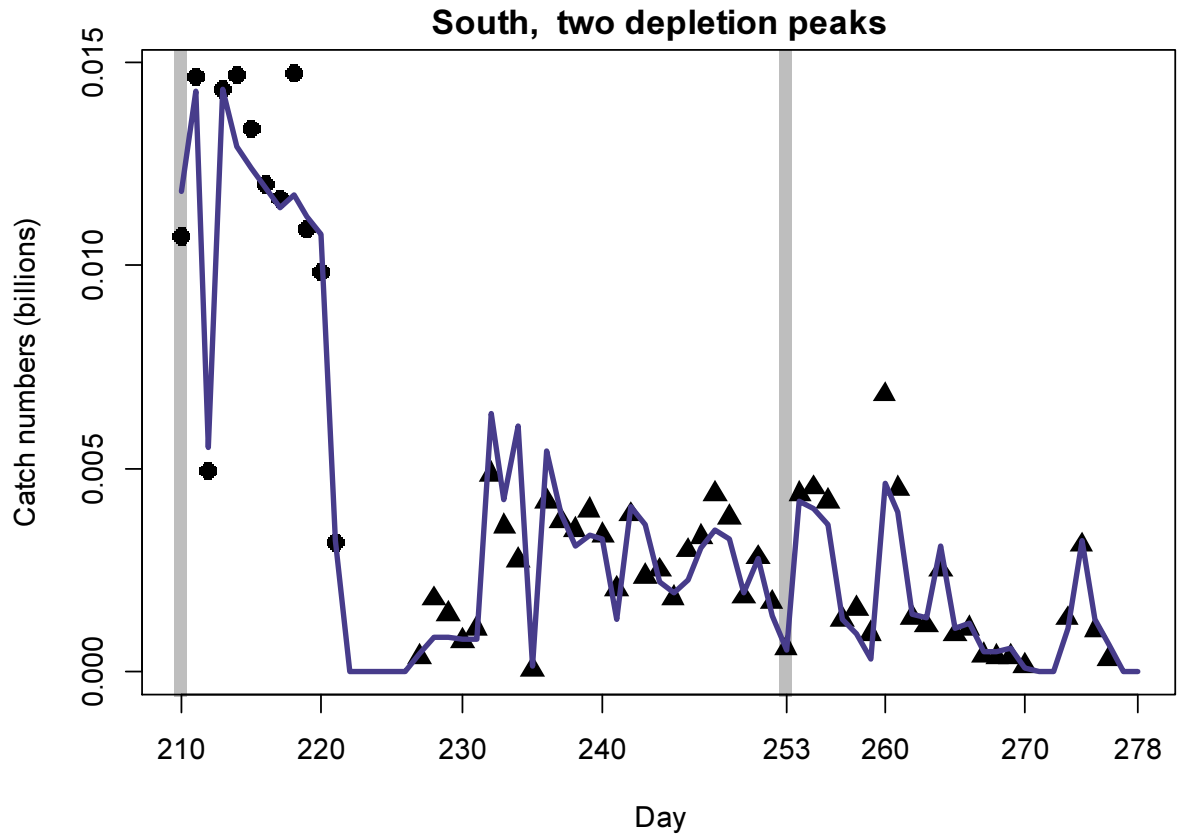
Figure A2-S [previous page – top]. Daily catch numbers estimated from actual catch (black points: without SEDs, black triangles: with SEDs) and predicted from the depletion model (purple line) in the south sub-area.

Figure A2-N [previous page – bottom]. Daily catch numbers estimated from actual catch (black points: without SEDs, black triangles: with SEDs) and predicted from the depletion model (green line) in the north sub-area.

For the north sub-area, joint optimization of Equations **4** and **5** resulted in parameters values:

Bayesian $N1_{N\ day\ 217}$ $= 0.258 \times 10^9$;   Bayesian $N2_{N\ day\ 258}$ $= 0.093 \times 10^9$

Bayesian $q_{N\ NSED}$ $= 0.881 \times 10^{-3}$ [n]

Bayesian $q_{N\ SED}$ $= 1.363 \times 10^{-3}$ **(A9-N)**

These parameters produced the fit between predicted catches and actual catches shown in Figure A2-N.

Natural mortality

Natural mortality is parameterized as a constant instantaneous rate $M = 0.0133$ day^{-1} (Roa-Ureta and Arkhipkin, 2007), based on Hoenig's (1983) log mortality vs. log maximum age regression applied to an estimated maximum age of 352 days for *Doryteuthis gahi*:

$\log(M)$ $=$ $1.44 - 0.982 \times \log(age_{max})$

M $=$ $\exp(1.44 - 0.982 \times \log(352))$

$=$ 0.0133 **(A10)**

Hoenig (1983) derived Equation **A10** from the regression of 134 stocks among 79 species of fish, molluscs, and cetaceans. Hoenig's regression obtained $R^2 = 0.82$, but a corresponding coefficient of variation (CV) was not published. A CV of M was estimated by measuring the coordinates off a print of Figure 1 in Hoenig (1983) and repeating the regression. Variability of M was calculated by randomly re-sampling, with replacement, the regression coordinates $10000\times$ and re-computing Equation **A10** for each iteration of the resample (Winter 2017). The CV of M from the 10000 random resamples was:

CV_M $=$ $SD_M / Mean_M$

CV_M $=$ $0.0021 / 0.0134 = 15.46\%$ **(A11)**

CV_M over the aggregate number of unassessed days between survey end and commercial season start was then added to the CV of the biomass prior estimate and the CV of variability in vessel catches on start day (**A5-S** and **A5-N**). CV_M was further expressed as an absolute value and indexed by sign($1 - CV_M$) to ensure that the value could not decrease if CV_M was hypothetically > 100% (**A5-S**).

---

[n] On Figure 8-left.

Total catch by species

Table A1: Total reported catches and discard by taxon during second season 2017 *Doryteuthis gahi* fishing, and number of catch reports in which each taxon occurred.

Species Code	Species / Taxon	Catch Wt. (KG)	Discard Wt. (KG)	N Reports
LOL	*Doryteuthis gahi*	24101290	12036	1002
PAR	*Patagonotothen ramsayi*	1129752	1122154	997
BLU	*Micromesistius australis*	298650	97546	312
RAY	Rajidae	98480	20847	627
BAC	*Salilota australis*	70525	8273	328
HAK	*Merluccius hubbsi*	60635	6388	469
WHI	*Macruronus magellanicus*	50397	21723	113
GRV	*Macrourus* spp.	35811	17946	308
MUN	*Munida* spp.	30544	30544	89
CGO	*Cottoperca gobio*	24054	22263	594
TOO	*Dissostichus eleginoides*	16530	4043	377
DGH	*Schroederichthys bivius*	6817	6816	230
SAR	*Sprattus fuegensis*	3194	3194	21
KIN	*Genypterus blacodes*	2392	1444	113
EEL	*Iluocoetes fimbriatus*	1834	1822	96
UCH	Sea urchin	1131	1131	30
DGS	*Squalus acanthias*	928	928	24
ING	*Moroteuthis ingens*	675	675	57
LAR	*Lampris immaculatus*	469	476	17
DGX	dogfish / catshark uid	449	449	12
POR	*Lamna nasus*	270	270	4
LIM	*Lithodes murrayi*	200	200	1
CHE	*Champsocephalus esox*	145	145	16
PAT	*Merluccius australis*	131	136	21
BDU	*Brama dussumieri*	118	118	29
SCA	scallop	83	83	8
MUL	*Eleginops maclovinus*	64	68	13
OCT	Octopus spp.	54	54	5
ILL	*Illex argentinus*	34	33	8
GYF	*Gymnoscopelus fraseri*	33	33	2
MED	Medusae sp.	30	30	1
MXX	Myctophid spp.	25	25	2
ALF	*Allothunnus fallai*	8	8	1
DIM	*Dissostichus mawsoni*	4	2	2
MYX	*Myxine* spp.	4	4	2
NEM	*Neophyrnichthys marmoratus*	3	3	1
MAR	*Martialia hyadesi*	2	2	1
SEP	*Seriolella porosa*	1	1	1
Total		25935766	1381913	1002